Stony Brook University

Response profiles of neurons of the rat serotonergic dorsal raphe nucleus during goal directed behavior

A dissertation Presented

By

Sachin Prakash Ranade

to

The Gradual School

In Partial Fulfillment of the

Requirements

For the Degree of

Doctor of Philosophy

in

Neuroscience

Stony Brook University

August 2007

Stony Brook University

The Graduate School

Sachin Prakash Ranade

We, the dissertation committee for the above candidate for the Doctor of Philosophy degree, hereby recommend acceptance of this dissertation.

Zachary F. Mainen - Dissertation Advisor
Associate Professor, Cold Spring Harbor Laboratory

Carlos Brody - Chairperson of Defense
Associate Professor, Princeton University

Karel Svoboda
Group leader, Janelia Farm Research Center

Anthony Zador
Professor, Cold Spring Harbor Laboratory

Mihaly Hajos – External member
Associate Research Fellow, Pfizer Inc.

This dissertation is accepted by the Graduate School

Lawrence Martin
Dean of the Graduate School

Abstract of the Dissertation

Response profiles of neurons of the rat serotonergic dorsal raphe nucleus during goal directed behavior

by

Sachin Prakash Ranade

Doctor of Philosophy

in

Neuroscience

Stony Brook University

2007

Serotonin is an important neuromodulator implicated in psychiatric disorders including anxiety, depression as well as a diverse range of physiological functions. Serotonin is released in the brain from neurons located in raphe nuclei, a set of neurons located in the brainstem. How do neurons in these nuclei sub serve these diverse functions? We sought to address this issue by recording activity of raphe neurons during a well defined behavioral task and correlating changes in activity with specific behavioral events.

We recorded neuronal activity from rats trained on a 2 odor discrimination task where they learned to associate odors to water reward at 1 of 2 locations. This simple task allowed us to test different hypotheses of serotonin function. During the stimulus sampling phase we could test the theory of sensorimotor gating; i.e. inhibition of raphe neurons during orientation to behaviorally relevant stimuli. Based on odor identity, the rat made a movement to the reward location, thus enabling us to identify movement related responses. A small subset of randomly selected correct responses was not rewarded. This

allowed us to test the prediction that raphe neurons may encode an outcome that was worse than expected i.e. a disappointment signal. Introduction of a waiting time between response and reward delivery gave us a way to identify responses encoding the expected time of reward.

We found that raphe neurons showed a remarkable diversity of basal firing properties as well as firing rate modulation during various phases of the task. Most neurons responded to one or more behavioral events. A large fraction of neurons inhibited their firing during stimulus sampling consistent with predictions. Notably, a large proportion also responded to the click of the water valve. A small subset of neurons showed changes in firing rate during unrewarded trials consistent with encoding disappointment. Some neurons encoded odor identity, direction of movement as well as time of expected reward. The diversity of response profiles suggests a complex role for raphe neurons in affecting different behaviors. This thesis opens up a promising avenue for research into serotonin function by using neuronal recordings during specific behavioral tasks.

Table of contents

List of figures

Acknowledgements

I joined the Neuroscience program at Stony Brook University in the fall of 2000 with no clue about Neuroscience! I thank my undergraduate teacher Milind Watve who inspired me to take an adventurous route in science. I also thank the teachers and classmates at Stony Brook who made it an exciting place to learn.

I would like to thank Zach for being an excellent mentor. His passion for science is infectious. He allowed me to independently explore what I wanted to do but was always available for practical guidance. He is an incredible stressbuster and it is always calming to talk to him before deadlines to gain perspective. I enjoyed my time immensely in his lab.

I thank my lab members both past and present, Veronica, Adam, Clau, Hatim, Gidon, Masa, Ninglong, and Matt for making the lab a fun place. I thank Mike, Clau for teaching me the technique of tetrode recordings, Nao for his suggestions, and Adam for his scientific fervour. I learnt a lot from them. Thanks are due to Barry who actually runs Marks building and Rob with whom I had lot of fun building stuff.

A special thanks to my committee members, Tony, Carlos and Karel who were very helpful, took interest in my work and offered good advice. I would like to thank Mihaly Hajos who agreed at a very short notice to be an external member on my committee. His feedback was very important to me.

I would also like to thank my family for their love and support. Finally, I thank my loving wife Anagha, with whom I began this perilous journey of graduate life. She has toggled endlessly and effortlessly between numerous roles those of wife, friend, support, philosopher, and guide. She always helped me to

pause and look at the big picture and nudged me when I needed a push toward my goal. It would have been an impossible journey without her love and support and I thank her for that.

Introduction

Serotonin is an important neuromodulator involved in a diverse range of physiological functions and behaviors as well cognitive and psychiatric disorders including depression and anxiety. Serotonin or 5-hydroxy tryptamine was discovered as a serum factor that led to constriction of blood vessels, hence the name ('sero' for serum and 'tonin' for increasing muscle tone). Evidence for the existence of serotonin as a neurotransmitter in the central nervous system came through fluorescent histological observation of serotonin in cell bodies and axon terminals in the brainstem (Dahlstrom and Fuxe 1964). Serotonin is released in the brain from neurons residing in a set of nuclei in the brainstem, called the raphe nuclei.

The word 'raphe' is derived from the Greek word 'rhaph' meaning seam or suture, on account of the medial location of serotonin neurons in the brain. The raphe nuclei are the medial most nuclei of the reticular formation and stretch along the rostro-caudal extent of the brainstem. Raphe nuclei are evolutionarily conserved across fish, amphibians, up to mammals. Raphe nuclei are extremely heterogeneous with distinct neuronal morphologies, neurochemistry and diverse projections throughout the central nervous system and spinal cord.

Anatomical organization of raphe nuclei

Raphe nuclei are classified into rostral and caudal group of nuclei depending upon their anatomical location(Tork 1990). The caudal group resides in the medulla oblongata and caudal pons and mainly sends descending projections to the spinal cord. These nuclei are collectively referred to as medullary raphe nuclei and include three separate clusters of neurons, namely

raphe magnus, raphe pallidus, and raphe obscurus. The rostral group of nuclei resides in the caudal midbrain and the rostral pons and send ascending projections to the forebrain(Ungerstedt 1971). These include the dorsal raphe nucleus (DRN) and the median raphe nucleus (MRN), collectively referred to as pontine raphe nuclei. DRN and MRN send partially overlapping yet distinct projections to most areas in the forebrain(Molliver 1987). Although there are overlapping projections, DRN projects extensively to frontal cortex and striatum, while MRN preferentially innervates hippocampus and septum. This dual forebrain innervation is also anatomically distinct such that DRN axons are thin with pleomorphic varicosities while MRN axons are thicker with beaded varicosities(Kosofsky and Molliver 1987). DRN axons are differentially sensitive to neurotoxic amphetamine derivatives(Mamounas and Molliver 1988).

DRN is the major source of serotonin in the forebrain with the highest density of serotonin neurons. In the rat there are approximately 10,000- 12,000 serotonin neurons in the DRN which constitute 30% of neurons in this nucleus. The total number of serotonin neurons in all nuclei is estimated to be approximately 20,000-25,000(Jacobs and Azmitia 1992; Adell, Celada et al. 2002). Thus, the DRN constitutes approximately 50% of all serotonin neurons in the brain.

Afferents to the DRN

The DRN receives diverse inputs from cortical, limbic and brainstem structures. It receives a very strong input from the lateral habenula, as well as extensive projections from various cortical areas including lateral and medial orbital cortex(Aghajanian and Wang 1977; Hajos, Richards et al. 1998), infralimbic, insular cortices as well as preoptic and hypothalamic areas(Peyron, Petit et al. 1998). Moderate density of projections is seen from the central nucleus

of the amygdala. There are less dense projections from areas in the basal forebrain such as the lateral septum. There is evidence for a rough topographic distribution of afferents such that different regions innervate specific sub regions of the DRN(Peyron, Petit et al. 1998; Abrams, Johnson et al. 2004). Thus, amygdala projections chiefly innervate the central DRN while various cortical areas preferentially project to different subdivisions within the rostral part of the DRN.(Jacobs, Foote et al. 1978)

Inputs to the DRN show neurochemical heterogeneity. It includes dopaminergic and GABAergic inputs from the ventral tegmental area and substantia nigra(Kalen, Skagerberg et al. 1988; Kirouac, Li et al. 2004), noradrenergic inputs from the locus coeruleus, cholinergic afferents from the diagonal band of Broca, neuropeptides from the periaqueductal gray and hypothalamus(Jacobs and Azmitia 1992).

Projections of the DRN

The DRN sends extensive projections to diverse areas of the forebrain including the limbic system, hypothalamus, basal ganglia and cortical areas(Tork 1990), making it the most widespread neuromodulatory system in the brain. Dense projections are found to the periaqueductal grey, VTA, intralaminar thalamic nuclei, amygdala, hippocampus, striatum, hypothalamic and preoptic areas(Kalen, Karlson et al. 1985; Vertes 1991). It also sends projections to cortical regions. In addition the DRN sends axon collaterals to itself, thus generating a strong feedback loop(Mosko, Haubrich et al. 1977; Jacobs and Azmitia 1992). It also projects to the MRN. Similar to afferents, projection patterns also have been shown to have an organized distribution. Thus, hippocampal projections arise mainly from the caudal DRN while the cortical projections arise mainly from the rostral DRN(Imai, Steindler et al. 1986; Vertes 1991). Similarly, double and triple

labeling studies in functionally related areas have demonstrated that the same DRN neuron sends collaterals to innervate parts of a functional circuit (Imai, Steindler et al. 1986; Lowry 2002).

Heterogeneity of neuron types in the DRN

In addition to the complex organization of inputs and outputs, the DRN itself is highly heterogeneous with respect to its internal organization. While raphe nucleus is synonymous with serotonin, serotonergic neurons only form about 1/3rd of the neurons in the nucleus. In addition to serotonin, there are neurons that secrete GABA, dopamine, nitric oxide, and a variety of neuropeptides such as galanin, somatostatin(Araneda, Gysling et al. 1999). Similarly, with respect to firing properties numerous studies have reported a wide variety of neuronal firing patterns in the DRN(Kocsis and Vertes 1992; Allers and Sharp 2003; Kocsis, Varga et al. 2006). Neuronal subpopulations have been identified that respond differently to changes in animal state from awake state to sleep (Sakai and Crochet 2001; Urbain, Creamer et al. 2006). Thus, there is an incredible morphological, neurochemical, anatomical and functional heterogeneity in the DRN.

Theories of serotonin function

Serotonin is involved in diverse behaviors and physiological conditions including anxiety, satiety, depression, aggression, motor control, rhythmogenesis, impulsivity, learning, sleep disorders, and social dominance. While all these effects of serotonin dysfunction are well known, a global theory of serotonin function does not exist. I will outline some of the major theories that have been put forth in the field.

Motor hypothesis/sensorimotor gating hypothesis

An extensive set of recordings conducted in the freely behaving cat, led Barry Jacobs and his colleagues at Princeton to postulate the motor hypothesis of serotonin function(Jacobs and Fornal 1999). Their results indicated that serotonin neurons in the DRN were remarkably non-responsive to aversive and stressful stimuli. On the other hand these neurons responded during movement including rhythmic movements such as licking, whisking, grooming etc. In response to orienting stimuli such as sudden opening of the door of the recording room, these neurons abruptly fell silent. On the basis of these observations, they proposed that serotonin neurons tonically inhibit sensory processing and facilitate motor output. However, when the animal needs to attend to a stimulus, these neurons are inhibited thereby disinhibiting processing of behaviorally relevant sensory information and disfacilitating motor output. This is how they explain the pause in activity of neurons during the door opening. While this theory is supported by many anecdotal observations such as the pause in activity of the 'door opening neuron' these data are anecdotal at best and requires rigorous testing. Thus, the DRN is inhibited while attending to relevant stimuli. It can be postulated that the opposite would be true for irrelevant, distracting stimuli; i.e. serotonin will be released in response to such stimuli. In support of this argument, it has been found that serotonin administration into the forebrain leads to inhibition of the acoustic startle reflex, a response to distracting irrelevant stimuli (Davis, Strachan et al. 1980). Thus, serotonin may aid in suppressing the processing of the irrelevant stimulus. This theory goes hand in hand with the theory of behavioral inhibition. The sensorimotor gating hypothesis accounts for some of the effects of serotonin and firing properties of serotonin neurons. However, it does not account for the major deficits seen in reinforcement learning. There are 2 major effects of serotonin depletion on

aspects of reinforcement learning, namely discounting of delayed rewards, and aversive reinforcement.

Delay discounting and temporal differentiation

Delay discounting is referred to devaluation of value of delayed rewards. Rats can learn the value of delayed rewards and use it to make decisions. In a classic delay discounting paradigm, rats have to choose between a small immediate reward and a large delayed reward. The reward magnitude and delays are then titrated to reach a stable point where they are chosen with equal probability. With serotonin lesions rats become excessively sensitive to reward delay and prefer to choose the small immediate reward(Mobini, Chiang et al. 2000). On the basis of these findings, Kenji Doya has proposed a general function for serotonin as setting the parameters of the delay discounting function.(Doya 2002). In another timing based behavioral paradigm rats have to make an operant response only after a certain fixed time interval 't' in order to receive reward. Premature response reset this requirement. Again, with serotonin lesions rats tend to make the more premature responses. Thus, there is a general inability to withhold responding coupled with a change in the perception of time(Ho, Velazquez-Martinez et al. 2002). Thus, serotonin is intricately involved with timing of behavioral response.

Serotonin as a punishment signal

Serotonin lesions lead to marked impairments in reinforcement learning. Rats are unable to learn a simple go no-go behavior(Harrison, Everitt et al. 1999). This is related to deficits in withholding a response, a conclusion that has led to the proposal of serotonergic involvement in behavioral inhibition. At the same time, serotonin is also involved in learning about aversive reinforcers or

punishments. These 2 findings go hand in hand. i.e. learning about bad things, and staying away from them both require serotonin. These roles are exactly opposite to the known effects of dopamine eliciting Pavlovian approach behavior and its involvement in reward processing. It has also been shown by Schultz's work that dopamine neurons encode the positive error in prediction of expected rewards(Hollerman and Schultz 1998). Based on these opponent interactions and Schultz's findings, Peter Dayan and colleagues proposed that serotonin encodes a negative prediction error signal; i.e. it indicates worse than expected outcomes (disappointment)(Daw, Kakade et al. 2002).

Disconnect between behavioral effects of serotonin and raphe neuronal responses

While there are diverse effects of serotonin on various behaviors as was described in the earlier section, recordings from serotonin neurons in the raphe nucleus have yielded very different results. The main findings of the few studies conducted in awake animals is the tonic modulation of firing rates across the sleep wake cycle and general correlations with motor movements dictated by level of arousal(Fornal, Metzler et al. 1996). While these recordings have been fundamental to our understanding of raphe circuitry, they have not in any way addressed the forebrain effects of serotonin. We feel that the main reason for this is the absence of well controlled behavioral assays.

Recording activity during behavioral task

Recordings in animals performing well controlled behavioral tasks have been instrumental in advancing our understanding of brain systems. One of the prime examples of the success of this approach is seen in the dopamine system. It was known for a long time that dopamine is involved in reward learning and

approach behavior(Schultz and Romo 1990). However, it was only after Schultz and colleagues recorded the activity of dopamine neurons in the VTA and substantia nigra during pavlovian conditioning paradigms did they find out that dopamine neurons encode reward expectation. Specifically dopamine neurons encode outcomes which were better than expected i.e. surprise or what is more formally referred to as reward prediction error(Mirenowicz and Schultz 1994; Hollerman and Schultz 1998).

There have been no recordings in the serotonin system from animals performing well controlled behavioral tasks. We believe that employing this approach in the raphe nucleus will help in increasing our understanding of serotonin function. The goal of this study was to record activity of neurons in the dorsal raphe nucleus during a temporally well –controlled two odor discrimination task to test various theories of serotonin function. Our task enabled us to specifically test the sensorimotor hypothesis of serotonin, negative prediction error hypothesis, and role of serotonin in encoding reward delays.

Firing properties of raphe neurons in awake rats

Introduction

The dorsal raphe nucleus (DRN) is the major source of serotonin to the forebrain and contains the largest concentration of serotonergic neurons. Still, these constitute only 30% of the neurons in this nucleus (Jacobs and Azmitia 1992). The remaining population of neurons is non-serotonergic and includes local and projection neurons. These may contain GABA, dopamine, nitric oxide, and various neuroactive peptides. Thus, the DRN is neurochemically and cytoarchitecturally diverse. Most electrophysiological studies have focused on characterizing the firing properties of putative serotonergic neurons. According to these studies, classical serotonergic neurons have a wide action potential waveform, regular firing pattern with narrow inter spike interval distribution, and low firing rates (~4 Hz during awake moving phase) that decrease further as the animal transitions from awake state to sleep and completely cease firing in REM sleep(McGinty and Harper 1976; Trulson and Jacobs 1979; Levine and Jacobs 1992). They inhibit firing upon administration of 5HT1a receptor agonists via an inhibitory feedback mechanism through somatodendritic 5HT1a autoreceptors(Trulson and Crisp 1986; Sprouse and Aghajanian 1987). Recently, there have been reports that conclusively demonstrate subpopulations of serotonin neurons that do not conform to these criteria. Thus, there are non-wide spiking serotonin neurons(Allers and Sharp 2003),serotonin neurons without clock-like firing pattern (Kocsis, Varga et al. 2006; Hajos, Allers et al. 2007) and also neurons that are unresponsive to 5HT1a agonists(Veasey, Fornal et al. 1995; Sakai and Crochet 2001). Similarly, within the wide spiking neurons a large

diversity of basic firing properties has been reported(Sakai and Crochet 2001; Urbain, Creamer et al. 2006). There are only few studies recording firing properties of putative non-serotonergic neurons. In the awake rat, narrow spiking neurons were recorded along with hippocampal theta rhythm(Kocsis and Vertes 1992). A heterogeneous population was found with slow, medium and fast firing neurons with firing rates ranging from <10 Hz to greater than 55 Hz. More than 50% of these neurons showed correlation of firing with the hippocampal theta rhythm.

In this section, I will briefly describe the recording approach, and elaborate on basic firing properties of dorsal raphe neurons in the freely behaving rat.

Recording setup

The dorsal raphe nucleus (DRN) is located at 7.6mm posterior to bregma along the midline at a depth of 5mm from the surface. This stereotactic location is directly below the confluence of the sagittal and transverse sinus. A procedure was developed to target tetrodes to the DRN through a guide cannula (See Materials and Methods, guide cannula implantation; Fig 2-1A). A microdrive was designed specifically to allow access to the brain through the cannula, circumventing the sinus (See Materials and Methods, microdrive design, Fig 2-1B). Using this approach, we recorded the activity of 50 neurons in the DRN of 7 rats in 26 sessions. (See Materials and Methods, tetrode recordings; Fig 2-2). Extracellular waveforms were recorded and separated into distinct sources (i.e. units/cells/neurons) using manual spike sorting (see Methods). Position of recording site within the DRN was histologically confirmed after termination of the experiment (see Fig 2-1 C). Data was collected from a total of 12 rats. However, DRN was determined to be targeted in only 7 rats which are included

in the analysis. Cells from different sub regions of the raphe nucleus have been pooled for the present analysis.

One of the advantages of using multi-channel tetrodes as recording electrodes is that it allows improved isolation of multiple neurons simultaneously. However, in the DRN mostly single units were isolated (Mode = 1). A maximum of 3 well isolated units was obtained. The low yield may be attributed to absence of layered organization and therefore lower local cell density compared to cortical and hippocampal areas. It was observed that overall neural (electrical) activity fluctuated through the depth of the DRN with small areas of high activity interspersed with stretches of relative electrical silence.

Waveform classification

One of the standard definitions of serotonin neurons is their broad action potential waveform with a very large hyperpolarization phase(Aghajanian and Vandermaelen 1982; Jacobs and Fornal 1991) whereas nonserotonergic neurons have a narrow spike waveform. This simple view has been challenged by other studies that have shown presence of narrow spiking serotonin neurons as well as a general a diversity of waveforms. Most previous recording studies have focused on specific neuronal populations based on waveform shape as well as other firing properties(Fornal, Metzler et al. 1996).

We did not use any pre-selection criteria for our recordings. In our dataset, we observed a large variety of waveform shapes. Waveforms differed in more than one feature and were intially classified visually into 13 subclasses. However, to gain a better quantitative handle on the classification and reduce the number of classes, we measured a number of features of spike waveforms, namely amplitude of peak, amplitude of pre-valley and post-valley, hyperpolarization, width and repolarization. From these measurements we also

calculated derived measures such as repolarization, Valley-Valley2 ratio (VV2 ratio), Peak-Valley2 ratio (PV2 ratio) as shown in Fig 2-3). While most properties were distributed as a continuum, the Peak Valley2 ratio property had a bimodal distribution. We used this property along with VV2 ratio and hyperpolarization to divide all cells into 3 classes. Fig 2-4A plots the 2 properties for all neurons. Our classification scheme is adapted from Urbain, Creamer et al 2006 who classified neurons based on spike width and peak – valley ratio. We classified all neurons into 3 classes. Asymmetric broad spiking neurons had high PV2 ratio and high hyper polarization. Symmetric neurons had low PV2 ratio and a variable hyperpolarization value. A third class of triphasic neurons did not fit any other waveform class on account of a high pre-valley. This class was combined with the symmetric neurons for further analysis. Average waveforms for each class are plotted in Fig 2-4B. Henceforth, asymmetric wide spiking neurons will be referred to as putative serotonergic neurons.

Classical wide spiking neurons

According to standard criteria, wide spiking neurons have regular, low firing rates, and show sleep – wake modulation of their firing rates. Fig. 2-5 shows an example of a classical putative 5HT neuron. It has a broad spike waveform, regular firing with a low covariance of 0.3. It also shows sleep wake modulation of its firing rate. Of the 13 neurons that were classified as wide spiking, 5 neurons fulfilled these criteria. They had a mean firing rate in the awake condition of 1.68 Hz (± 0.26) with a mean C.O.V of 0.22 (± 0.06). C.O.V. is defined as the variance of the inter spike interval distribution. A small variance is indicative of regular firing. Firing rate decreased during sleep epochs to an average of 70% (± 2%) of the awake firing rate. Thus we were able to identify classical putative serotonergic neurons in our recordings.

Burst firing wide spiking neurons

It has been known through the work of Mihály Hajós and colleagues that there is a subpopulation of wide spiking neurons that can fire spikes in burst mode. They have very similar characteristics as classical wide spiking neurons (Hajos, Gartside et al. 1995; Hajos, Allers et al. 2007). Burst firing serotonin neurons may be able to elicit robust release of serotonin in terminal fields, and thus it would be interesting to know the behavioral correlates of these neurons.

Three of the broad spiking neurons in our data had a burst-firing pattern. Fig 2-6 shows an example of a typical burst firing neuron. It has a low firing rate (mean 1.7 Hz) in the awake state and a C.O.V. of 0.2. It also showed sleep wake modulation with the firing rate decreasing during sleep epochs to 78% of the awake firing rate. The average firing rate of the 3 neurons was 1.16 (± 0.4) Hz with an average sleep modulation of 64% (± 1.1). One of the neurons had an irregular firing pattern with a C.O.V. of 4.3.

Narrow spiking neurons

The non-wide spiking neurons formed a loosely defined class of neurons with very diverse firing properties. Firing rates of most neurons were low, ranging from <0.1 Hz to a median firing rate of 0.2 Hz. There were only a few neurons firing at more than 10 Hz. This class of neurons also showed sleep wake modulation with a median sleep index of 0.7. There were also instances of opposite sleep wake modulation. i.e. firing rates during sleep were higher than in awake state. An example of such a neuron is shown in Fig 2-7.

In conclusion, a high degree of heterogeneity of firing patterns was observed in the DRN, consistent with recent reports from various labs (Kocsis and Vertes 1992; Urbain, Creamer et al. 2006; Hajos, Allers et al. 2007). Thus the

raphe nucleus has a complex circuitry with a high diversity of neuronal types. Further characterization of these neuronal types would help to determine the nature of interactions occurring within the nucleus.

Figure 2-1: Procedure for tetrode microdrive implantation

(A) Guide cannula implantation. A schematic of the guide cannula implantation procedure is shown. IT shows a coronal section through the DRN at -7.8 mm posterior to bregma. The guide cannula (grey) is inserted through the sinus up to a depth of 3 mm from the surface of the skull. The tetrode micro drive(blue) is lowered carefully through the guide cannula and secured. After recovery from surgery, tetrodes are advanced slowly until they reach the DRN.

(B) 6 – channel 3-D printed microdrive. Photograph of an assembled 3-D printed 6-channel microdrive is shown. The metal tube protruding at the base is inserted through the guide cannula. The drive consists of 6 independently adjustable tetrodes that can be advanced in increments of 40 μm.

(C) Histological confirmation of location. Coronal section through the DRN, clearly showing the track of an individual tetrode, passing through and terminating outside the DRN. Recordings from within the boundary of the nucleus are included in the analysis

A

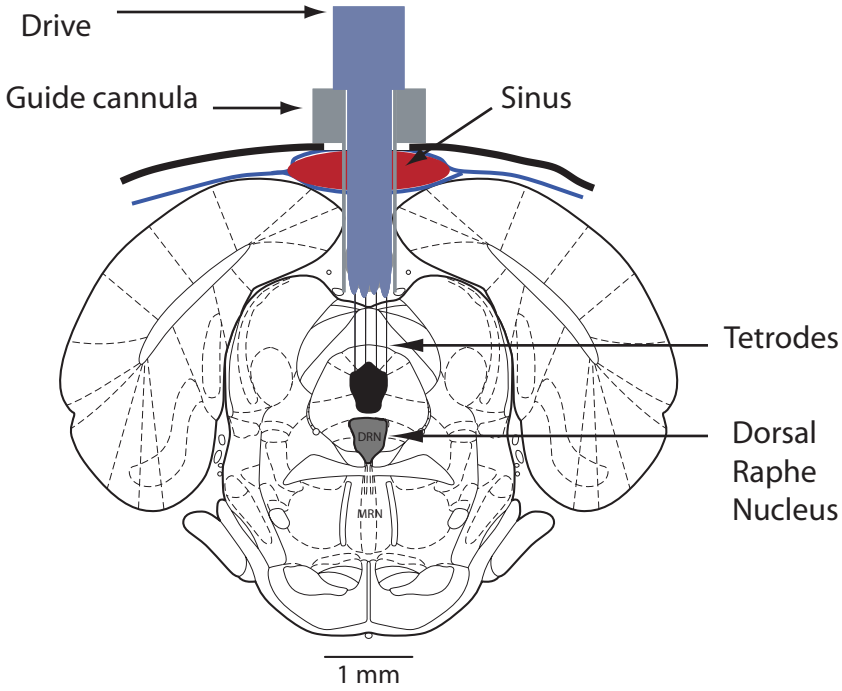

B

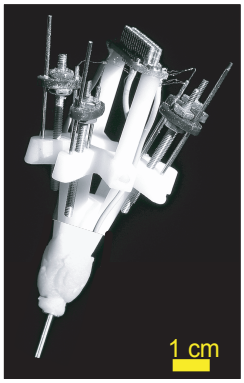

Tetrode microdrive

C

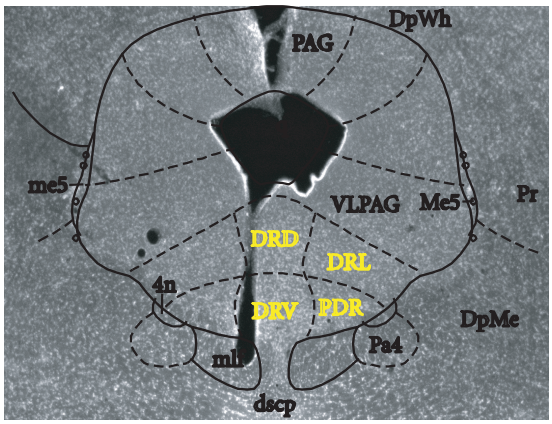

Bregma -7.68

0.5 mm

Figure 2-2: Spike sorting

(A) Plot of amplitude of events recorded on two channels of a tetrode. Points are assigned to 2 clusters. Multiple comparisons can be made using different waveform features in order to making distinct clusters. The black points represent noise spikes since they do not belong to any cluster.

(B) Spike waveforms from all 4 channels with average waveform, separated according to the clustering assignments. The 2 waveforms have very different shape as well as relative amplitudes on all channels.

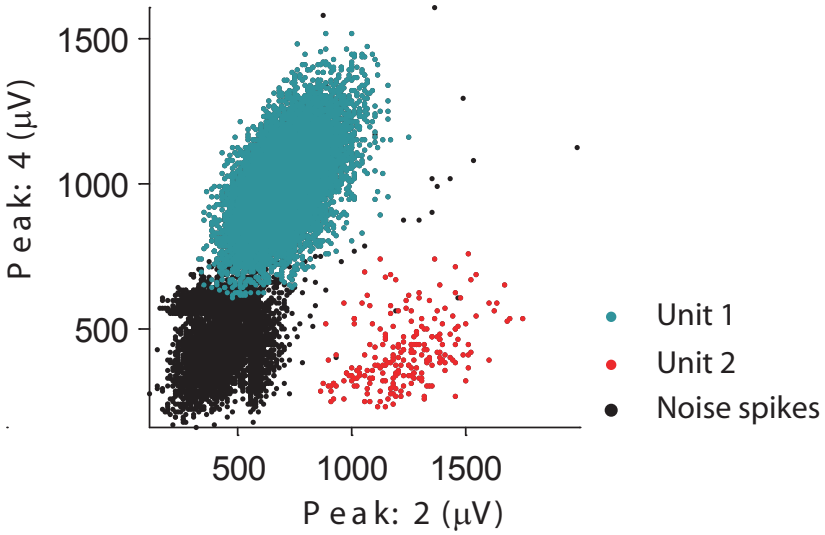
1500
1000
500
Peak: 4 (μV)
500
1000
1500
Peak: 2 (μV)
Unit 1
Unit 2
Noise spikes

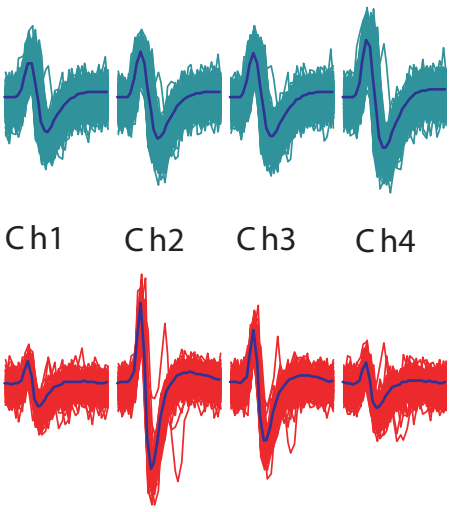
Ch1
Ch2
Ch3
Ch4

Figure 2-3: Spike waveform properties

(A) Example trace of an action potential waveform. The averaged waveform is shown for the cell. Features calculated for each waveform are represented. Peak is the amplitude of the positive deflection, Valley1 is the first negative deflection before baseline, Valley2 is the first negative deflection after baseline, width is the time between peak to valley , hyperpolarization is the time from start of valley 2 up to return to baseline.

(B) Distribution of spike waveform properties. Each panel shows the distribution of a waveform characteristic across 54 cells from the dorsal raphe nucleus. Properties are as defined in (A). Distribution of average firing rates during the entire behavioral epoch is plotted in lower right panel.

A

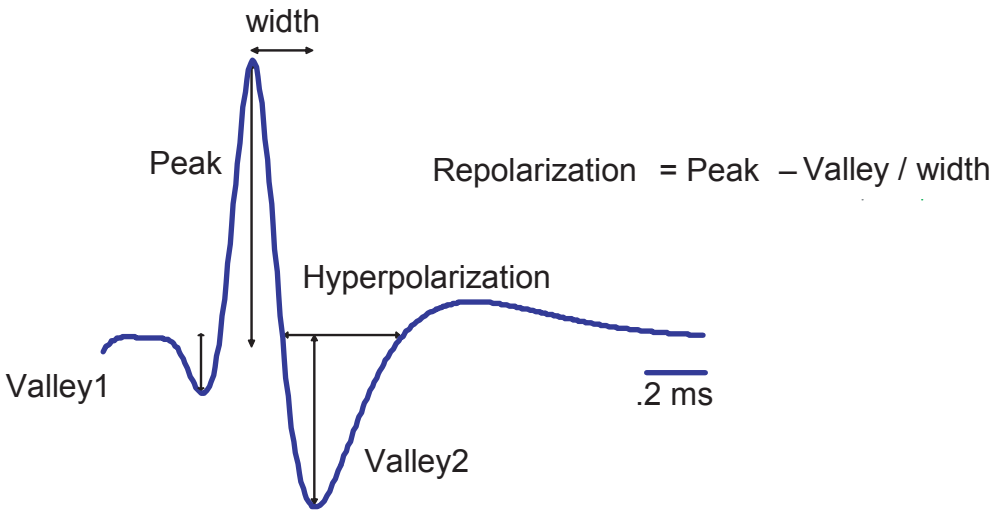
width
Peak
Repolarization = Peak – Valley / width
Hyperpolarization
Valley1
.2 ms
Valley2

B

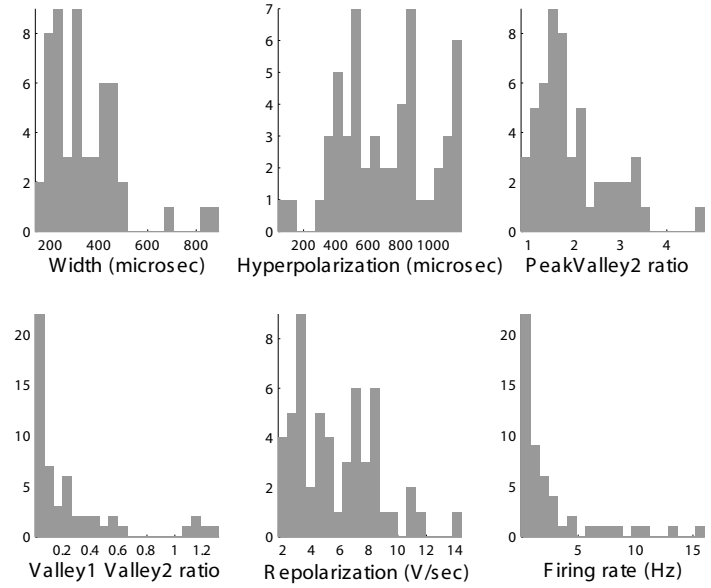
Width (microsec)
Hyperpolarization (microsec)
PeakValley2 ratio
Valley1 Valley2 ratio
Repolarization (V/sec)
Firing rate (Hz)

Figure 2-4: Cell classification based on spike waveform

(A) Scatter plot of hyperpolarization vs. Peak Valley2 (PV2) ratio. The two properties are positively correlated. On the basis of these 2 properties and the Valley1-Valley2 ratio (VV2) neurons were classified into 3 classes. Wide spiking neurons (blue, n =16) are characterized by high PV2 ratio and high hyperpolarization values. Narrow symmetric neurons (green, n=30) have low PV2 ratio and lower hyperpolarization values and triphasic neurons (red, n=5) are characterized by low VV2 ratios. Red cell shown with asterisk with low PV2 ratio is classified as triphasic neuron due to low VV2 ratio.

(B) Average spike waveform of 3 classes. Normalized average spike waveform for each class of neurons is shown.

A

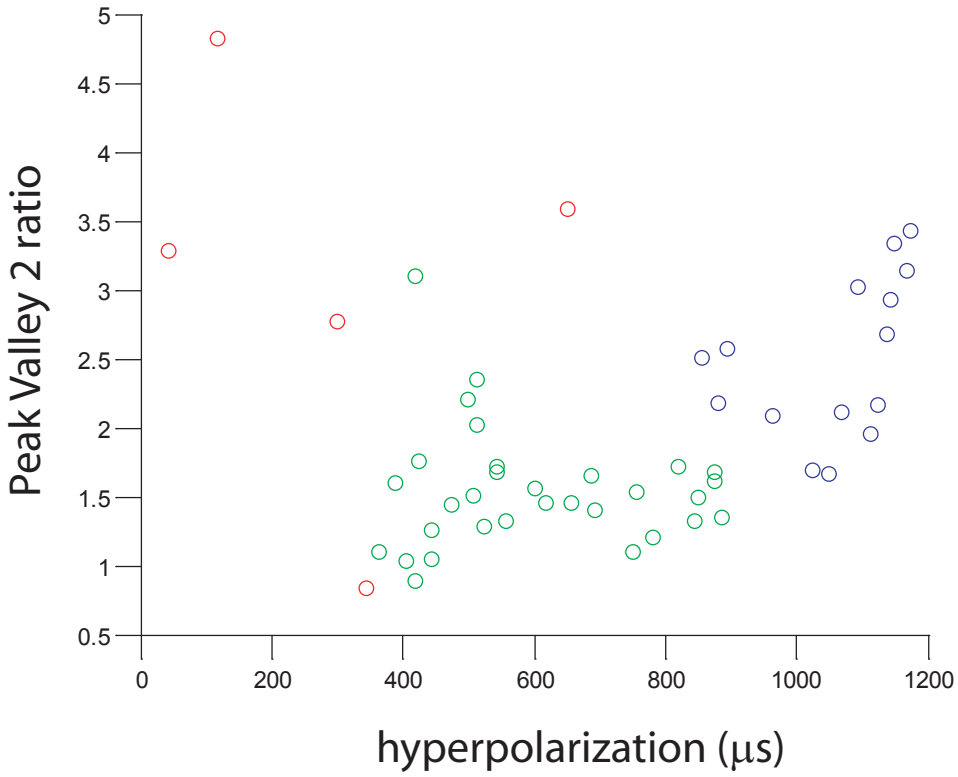
Peak Valley 2 ratio
5
4.5
4
3.5
3
2.5
2
1.5
1
0.5
0
200
400
600
800
1000
1200
hyperpolarization (μs)

B

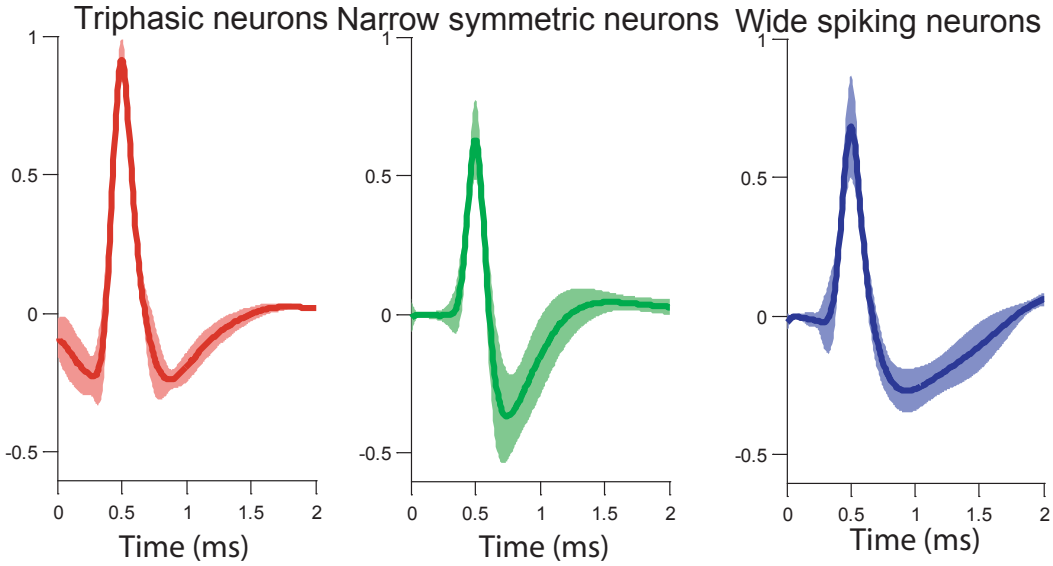
Triphasic neurons
Narrow symmetric neurons
Wide spiking neurons
1
0.5
0
-0.5
0
0.5
1
1.5
2
Time (ms)

Figure 2-5: Firing properties of wide spiking putative serotonerigc neuron

(A) Broad spike waveform of putative serotonergic wide spiking neurons is shown. Histogram of the log of the inter spike interval distribution is also shown.

(B) Sleep – wake modulation of firing rate. Fig. 2-6 B shows the spectrogram of the hippocampal EEG. Power in a frequency band is plotted according to color (blue is low power, red is high). An epoch of high power in the lower frequencies can be seen. This corresponds to a sleep epoch. Firing rate histogram shows a decrease in firing rate during the sleep epoch.

(C) Example traces of hippocampal EEG and spike train. Example traces of bipolar hippocampal EEG showing high amplitude oscillation. Spike train is plotted as black ticks.

(D) Average firing rates during sleep and wakefulness are plotted.

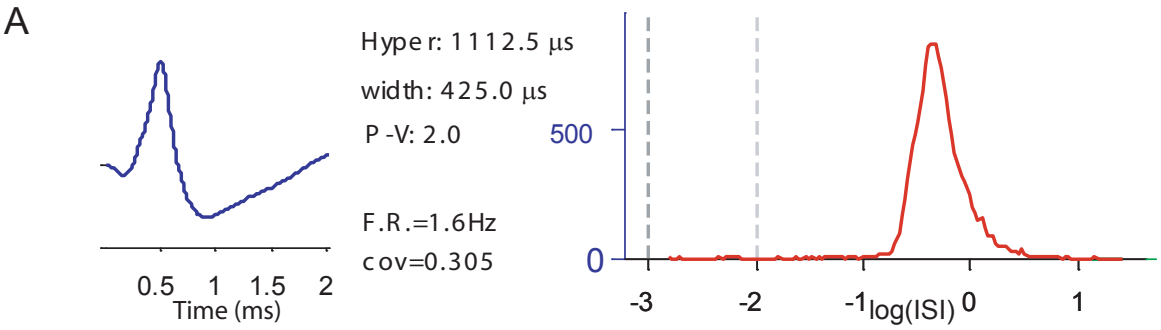
A
Hyper: 1112.5 µs
width: 425.0 µs
P-V: 2.0
F.R.=1.6Hz
cov=0.305
0.5
1
1.5
2
Time (ms)
500
0
-3
-2
-1
log(ISI)
0
1

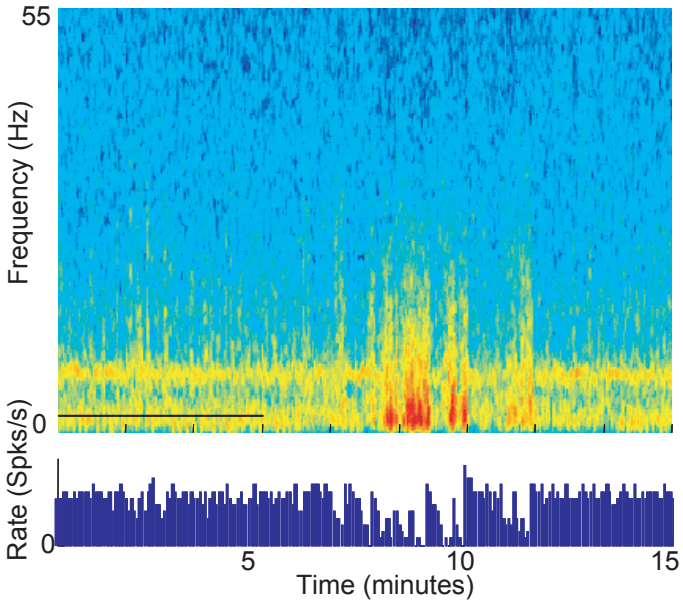
B
55
Frequency (Hz)
0
Rate (Spks/s)
0
5
10
15
Time (minutes)

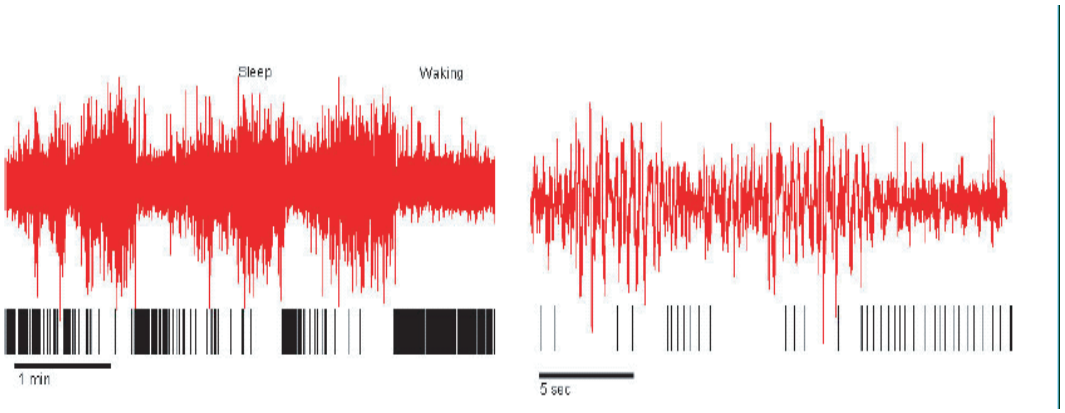
C
Sleep
Waking
1 min
5 sec

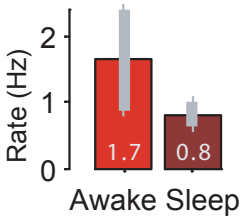
D
Rate (Hz)
2
1
0
1.7
0.8
Awake Sleep

Figure 2-6: Firing properties of burst firing wide spiking neuron

(A) Broad spike waveform of a burst firing wide spiking neurons is shown. Histogram of the log of the inter spike interval distribution is plotted. Note that the <10 ms bins contain spikes. These are the burst spikes with the low ISI.

(B) Sleep – wake modulation of firing rate. Spectrogram of hippocampal EEG is shown for 2 sleep epochs. Power in a frequency band is plotted according to color (blue is low power, red is high). An epoch of high power in the lower frequencies can be seen during each epoch. This corresponds to sleep periods. Firing rate histogram shows a decrease in firing rate during the sleep epochs.

(C) Example traces of hippocampal EEG and spike train. Example traces of bipolar hippocampal EEG showing high amplitude oscillation. Spike train is plotted as black ticks.

(D) Average firing rates during sleep and wakefulness are plotted.

A

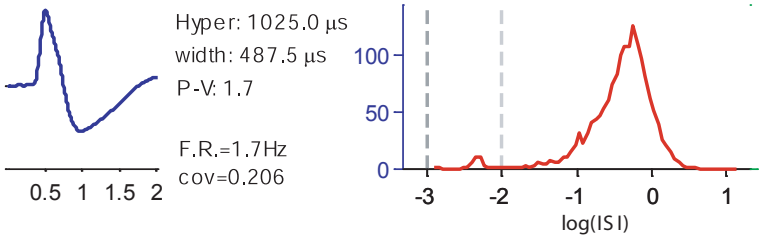
Hyper: 1025.0 µs
width: 487.5 µs
P-V: 1.7
F.R.=1.7Hz
cov=0.206
0.5 1 1.5 2
100
50
0
-3 -2 -1 0 1
log(ISI)

B

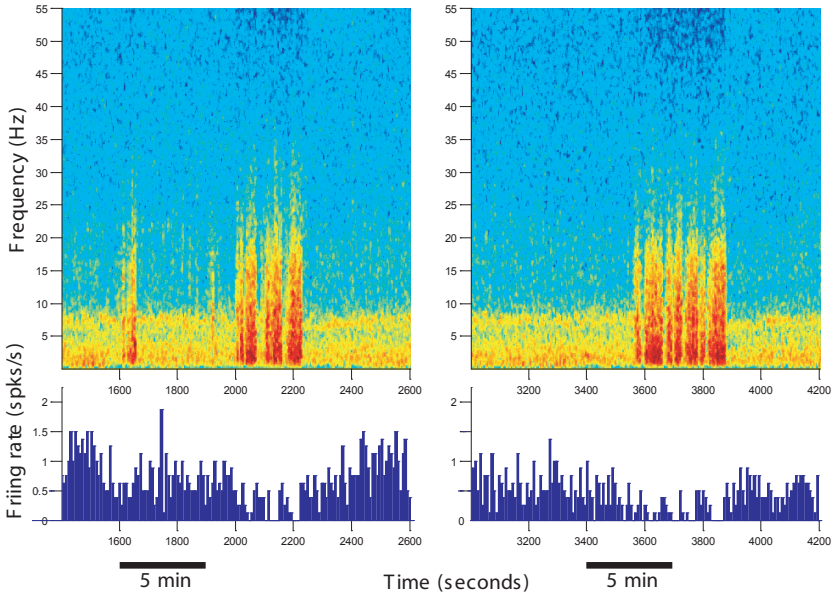
Frequency (Hz)
Friing rate (spks/s)
1600 1800 2000 2200 2400 2600
3200 3400 3600 3800 4000 4200
5 min
Time (seconds)
5 min

C

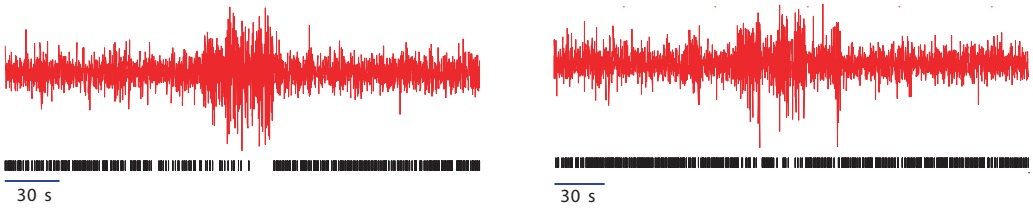
30 s
30 s

D

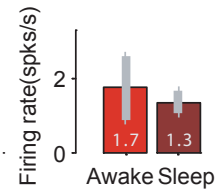
Firing rate(spks/s)
2
0
1.7
1.3
Awake Sleep

Figure 2-7: Firing properties of a non – wide spiking neuron

(A) Narrow spike waveform of a spiking neuron is shown. Histogram of the log of the inter spike interval distribution is also shown. It shows that this cell fires bursts and had a broad ISI distribution. i.e. irregular firing

(B) Sleep – wake modulation of firing rate. Spectrogram of hippocampal EEG is shown. Power in a frequency band is plotted according to color (blue is low power, red is high). An epoch of high power in the lower frequencies can be seen. This corresponds to sleep periods. Firing rate histogram shows an increase in firing rate during the sleep epochs.

(C) Example traces of hippocampal EEG and spike train. Example traces of bipolar hippocampal EEG showing high amplitude oscillation. Spike train is plotted as black ticks.

(D) Average firing rates during sleep and wakefulness are plotted.

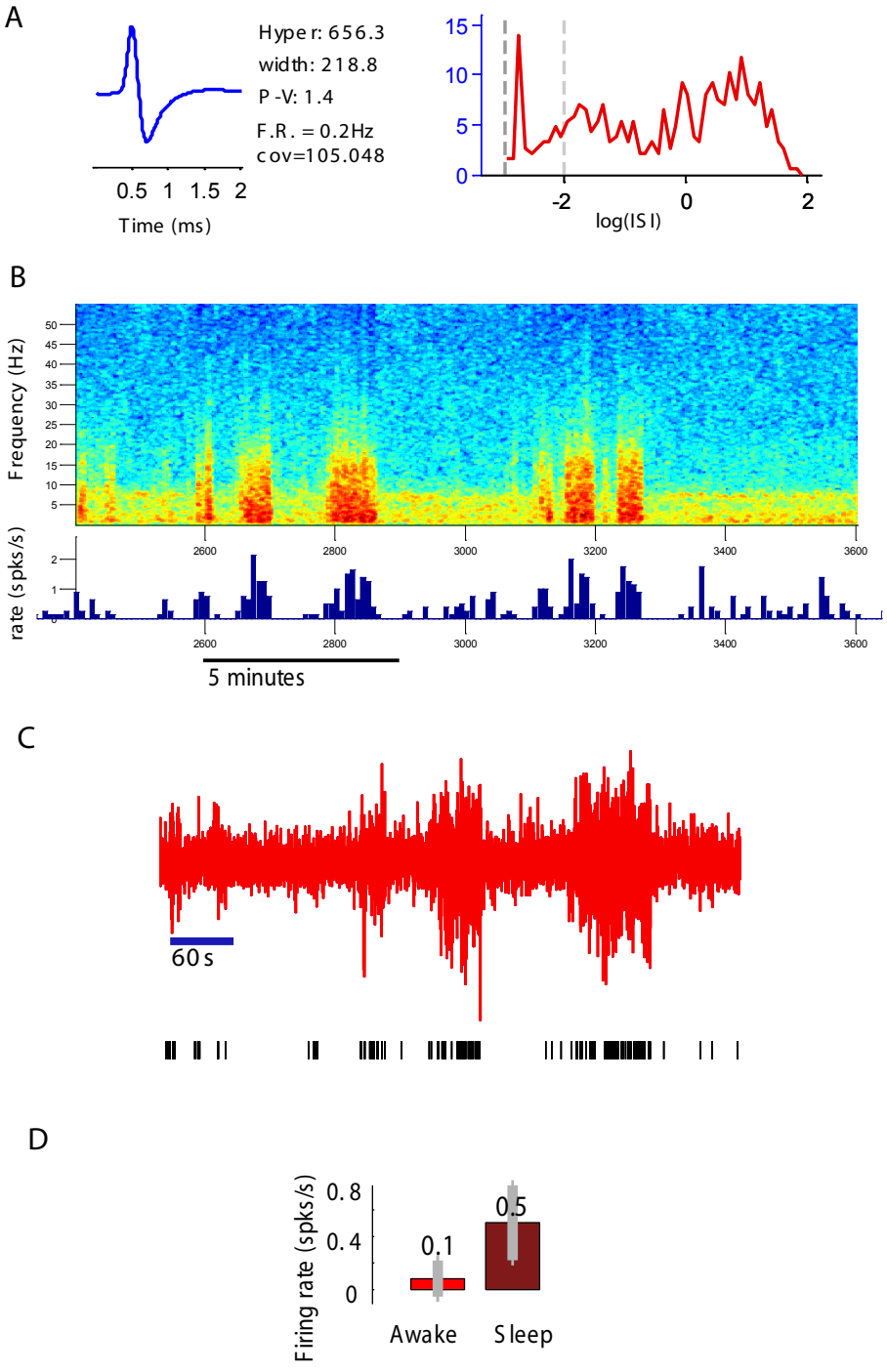
A
Hyper: 656.3
width: 218.8
P-V: 1.4
F.R. = 0.2Hz
cov=105.048
0.5 1 1.5 2
Time (ms)
15
10
5
0
-2 0 2
log(ISI)
B
Frequency (Hz)
50
45
40
35
30
25
20
15
10
5
rate (spks/s)
2
1
0
2600 2800 3000 3200 3400 3600
5 minutes
C
60 s
D
Firing rate (spks/s)
0.8
0.4
0
0.1
0.5
Awake
Sleep

Figure 2-8: Summary table of basic firing properties of wide spiking putative serotonergic neurons

The table summarizes basic firing properties of serotonin neurons.
Cellid is the database ID for that cell.
Hyperpolarization is the width of the hyperpolarization phase of the action potential waveform (see Fig. 2-1)
Awake firing rate is the average firing rate while the rat was neither sleeping nor doing the task.
C.O.V. is the variance of the inter spike interval distribution.
Sleep index is defined as Firing rate (Sleep)/ Firing rate (awake). – indicates that sleep information was not available for that cell.
Bursts indicate whether the neuron fired in bursts defined as an ISI of less than 10ms. – indicates no bursting.

No.	Cellid	Hyperpolarization (μs)	Awake firing rate (Hz)	C.O.V.	Sleep index	Burst
1	4	893	9.2	0.009	--	--
2	9	962	5.9	0.03	0.79	--
3	34	1168	3.8	0.03	--	--
4	38	1137	2.5	0.078	--	--
5	14	1068	2.1	0.149	0.48	--
6	39	1143	1.4	0.19	1.02	--
7	2	1025	1.7	0.2	0.78	1
8	18	1125	1.5	0.253	0.68	--
9	11	1112	1.7	0.3	0.49	--
10	12	1050	1	1.1	0.62	1
11	1	1093	0.8	4.3	0.54	1
12	7	881	0.5	11.7	1.01	--
13	17	856	0.5	20	--	--

Responses of raphe neurons during 2 odor discrimination task

Introduction

Serotonin is involved in a wide range of behaviors. On account of its diverse inputs as well as widespread projections to other brain areas, raphe neurons can influence different brain regions to affect a wide range of behaviors. DRN, with its large proportion of serotonin neurons is the major source of serotonin neurons in the forebrain. Thus, in order to understand the function of serotonin during behavior, it is important to study the firing properties of neurons in the DRN. In order to do this, we have recorded the activity of neurons in the DRN during the performance of a 2-odor discrimination task. In this section, I will describe the behavioral task in detail and outline task contingencies that allowed us to test specific hypotheses of serotonin function. I will describe correlates of raphe neuron firing during various phases of the task and the representation of behavioral variables. Finally, I will present evidence in support of the specific hypotheses being tested in the task, namely the sensorimotor gating hypothesis of serotonin function, negative prediction error hypothesis and encoding of reward delays by raphe neurons.

Two odor discrimination task

Rats have a well developed sense of smell and use their olfactory system to navigate their environment. Our lab has developed a 2 – odor discrimination paradigm that utilizes this natural ability of rats. In this task, a water deprived rat learns to associate a particular odor with availability of water reward at one of two locations. The behavior is easily trained, and rats perform more than 200

trials within a single behavioral session. In the basic task, the rat initiates a trial when it pokes its nose into a central poke (referred to as the 'odor port'). After a random delay to prevent motor stereotypy, 1of 2 odors is delivered into the odor port. The rat smells the odor and upon making its decision moves out of the odor port to either of 2 goal ports located to its left or right where a drop of water is delivered for choosing the correct port (Fig. 3-1). Thus, the task can be described a rule ('IF "ODOR A" GO LEFT, IF "ODOR B" GO RIGHT').

The 2-odor discrimination task is ideally suited to study neuronal correlates of behavior in the DRN, since it has sensory, motor, decision and reward phases and enables us to test specific predictions during every phase. We modified the basic 2-odor task so that we could test 3 specific hypotheses of serotonin function, namely motor hypothesis, serotonin as a source of negative prediction error signal and role of serotonin in temporal differentiation. I will now elaborate on these modifications.

(1) The motor hypothesis put forth by Barry Jacobs' group suggests that function of serotonin is to facilitate motor output and inhibit sensory processing. However, in the presence of a behaviorally relevant stimulus, raphe is inhibited to allow sensory processing. In the 2-odor discrimination task, the odor sampling period is when the rat needs to pay attention to the odor identity in order to make the correct response. Thus, we can assess the hypothesis of inhibition of DRN neurons during sensory acquisition i.e. odor sampling. The movement period allows us to look for movement related response of the same neurons. On the other hand, entry into the goal port necessitates the same movement without the stimulus. This provides an ideal control to exclude firing rate changes solely due to the motor action.

(2) Phasic serotonin has been postulated by Peter Dayan's group to encode a negative prediction error signal (i.e. signaling disappointment). We created a

mild disappointment situation by withholding reward on a small subset of randomly interleaved correct responses. Since rats were well trained on the reward contingencies, their expectation of the reward was high, therefore the manipulation should serve to create disappointment. According to the prediction of the theory, we expect to see a phasic increase in firing rate for trials where the reward was omitted compared to rewarded trials, or in a more general sense a differential response during unrewarded trials.

(3) Serotonin affects temporal regulation of behaviors, leading to the suggestion that it provides a timing signal(Ho, Velazquez-Martinez et al. 2002). In order to test the role of raphe neurons in encoding timing we introduced a long delay between entry into the goal port and reward delivery. We explicitly manipulated temporal reward expectation by keeping the reward delays fixed (1 sec) or drawing them from an exponential distribution (0.3 -2sec, mean 0.5). The fixed delay leads to explicit timing information. The exponential distribution on the other hand, leads to uniform expectation of reward in time on a given trial. However, it can lead to implicit temporal expectation shaped by previous experience. We predict that the reward delay or the rats' subjective temporal expectation of reward will be encoded in the firing rates. Such activity will be in the form of firing rate changes around the time of expected reward; e.g. sustained firing during delay period, increase or decrease in firing until the expected time of reward. Such responses can be studied by comparing firing rates in delay period in correct rewarded and unrewarded trials.

Task performance

Rats learned the task rapidly to reach a performance of up to 90% (Figure). Upon reaching criterion performance, they were surgically implanted with a microdrive in the DRN (see Materials and methods, surgical procedures). After

recovery from surgery, rats regained pre-surgery levels of performance (mean performance 86%). They typically performed a median of 190 trials (max: 706 trials; min 30 trials) within a behavioral session that lasted between 1-2 hours. Histograms of odor sampling duration (OSD) and movement time (MT) are plotted in Fig. 3-1. Rats were relatively fast in odor sampling (mean OSD = 0.44 sec). Typical movement times to go from odor port to the choice port were longer (mean MT = 0.81 sec). This may be due to restriction of movement due to recording cable and headstage. Slower movement times during recording sessions has been noted in earlier studies in our lab(Feierstein, Quirk et al. 2006). Video monitoring of behavior revealed extra delays caused by failure to immediately trip the infra-red beam recording time of goal port entry.

Modulation of firing rate during behavior

We recorded firing properties of 50 neurons in the DRN while rats were performing the 2-odor discrimination task. Four behavioral epochs were operationally defined for every trial. These were stimulus, movement, anticipation and reward/outcome. Most neurons (~85%) responded with a change in firing rate during at least one epoch. I will now describe neuronal correlates of behavior during these phases.

Odor port modulation

Upon entry into the odor port, there was a uniformly distributed random delay of 300-500 ms before odor onset. A large subset of neurons modulated their firing rate during this period (n = 30/54; ROC modulation index, $P<0.05$). ROC modulation index (RMI) was a measure of strength of modulation that was calculated by comparing distribution of firing rates during a baseline period with firing rates during the odor onset delay (See Materials and Method, ROC

analysis). Baseline was defined as a period of 500ms to 100ms before entry into odor port while the delay period was a period of 350ms immediately after odor port entry. Equal numbers of neurons were inhibited or excited. In some cases, firing ceased completely for a brief period of time (Fig 3-2A, left panel). Although this response profile was robustly seen in the dataset, no obvious correlation with waveform shape was observed. Fig. 3-2B shows distribution of RMI for all cells as a function of hyperpolarization. Cells with significant modulation are distributed uniformly as a function of hyperpolarization. Consistent with this finding, four cells with very different waveforms showed identical response profiles. Correlations with other responses were seen and will be described in later sections.

This is the first evidence we are aware of for inhibition of raphe neurons during stimulus sampling. The only evidence for inhibition during orientation toward a stimulus came from the observation of dorsal raphe neurons that paused firing when the door to the recording chamber was opened or closed and the cat oriented toward it(Fornal, Metzler et al. 1996). On the basis of this observation, they propose that the raphe is inhibited when the animal makes a purposive movement. Thus, inhibition while orienting to the stimulus is a direct demonstration of this hypothesis. We think this is not a motor response since it is not seen when the animal pokes its nose into the identical choice ports.

Odor responsive neurons

Serotonin inhibits sensory processing (Monckton and McCormick 2002). There are extensive projections from the DR to the olfactory bulb as well as other olfactory areas (Mamounas, Mullen et al. 1991). Barry Jacobs has noted that raphe neurons respond when the cat smelled food(Fornal, Metzler et al. 1996). We therefore expected to see odor responses of DRN neurons. After a random

odor onset delay, One of two odors was delivered in a carrier stream at a flow rate of 1L/min. The two odors used in this study were a 95:5 air mixture of (+) and (-)-2-octanols diluted 10-fold in mineral oil. Enantiomers of 2-octanol have similar smell as well as physical properties such as volatility yet can be easily distinguished by rats (Uchida and Mainen 2003). In a few behavioral sessions dilutions of pure enantiomers were used in place of mixtures. A total of thirteen neurons responded to the delivery of the odor stimulus with an abrupt increase in firing rate. The modal latency was ~200 ms (Fig. 3-3A). However, two cells recorded on the same tetrode, showed a latency of 40 and 20 ms (Fig. 3-3B). Six out of thirteen odor responsive neurons were selective for only one of the two odors ((Fig. 3-4). The average latency of odor response was 150 – 200 ms. A subset of neurons (15 of 50) was also inhibited during odor sampling, however, in most neurons inhibition was not specific to the sampling period. Four neurons showed a specific inhibition during odor sampling.

Apart from the two neurons that showed a very fast odor response, the odor response latency was relatively slow, raising the question of whether these responses are purely sensory or whether there is a sensorimotor component.

Movement responsive neurons

One of the major theories of serotonin function borne out of recordings is the motor hypothesis of serotonin (Jacobs and Fornal 1997; Veasey, Fornal et al. 1997; Jacobs and Fornal 1999). Results of extensive recordings performed in the awake cat, led Jacobs and colleagues to propose that the primary function of serotonin was to inhibit sensory processing and promote motor output. As has been outlined in the previous section, one of the most robust responses was an inhibition during odor sampling (i.e. sensory stimulus acquisition). We next looked for responses during the movement period.

The rat made a voluntary movement out of the odor port to one of two goal ports. ROC modulation index was computed during this phase by comparing firing rate during a fixed movement period of 300 ms to the pre-task baseline period. 30 neurons showed significant modulation of firing rates during this epoch with an equal number of neurons being inhibited and excited (Fig. 3-5A). While the inhibition was mostly locked to movement out of the odor port, increase in firing rate was observed at different latencies as is shown in Fig. 3-6. This may correspond to different parts of the movement, i.e. early withdrawal of head from the port versus head direction change toward the choice port. Similar to the odor sampling epoch, there was no correlation between modulation strength and waveform properties (hyperpolarization) (Fig 3-5B). Earlier studies have reported locomotion related cells in the raphe(Fornal, Metzler et al. 1996; Waterhouse, Devilbiss et al. 2004). Waterhouse et al reported non-serotonergic neurons to be related to movement. Thus, our finding that the movement related modulation was not correlated with spike width is consistent with these findings.

Direction selectivity

Ten out of the 30 movement responsive neurons were selectively tuned to direction of movement. Of this 1 neuron had opposite tuning to direction i.e. firing rate increased in one direction and decreased for the other direction. Example neurons are shown in (Fig. 3-6). Since rats were well trained they made very few errors. Therefore it was not possible to assess if the selectivity was truly for direction or an encoding of a combination of stimulus and response location.

While movement related responses have been well documented in raphe neurons, this to our knowledge is the first report of direction selective response in the dorsal raphe nucleus. It is conceivable that the direction selectivity is only

in the context of the task and is not generalized in all contexts. However, this remains to be tested.

Anticorrelation between odor port and movement response

It was observed that in a subset of neurons firing rate was modulated in opposite directions during odor sampling and movement. Examples of such opposite tuning are shown in Fig. 3-7A. Thus, a neuron that was inhibited during odor sampling fired more during movement and vice versa. This effect was quantified for all cells by comparing the modulation strength during the odor delay period with the modulation index immediately after exit from the odor port (Fig 3-7B, see schematic for epoch comparisons). A large fraction of neurons (n =30 out of 50), showed this property and a significant negative correlation (cc = -0.43; $P<0.04$) was obtained. However, there was no correlation of response type with spike width.

This finding gives further support to the motor hypothesis of serotonin. According to this hypothesis, raphe is inhibited during orientation to a relevant stimulus. Thus, our observation of cells being oppositely tuned during sensory and motor phases of the task provides a circuit level framework to generate a mechanistic model for the role of raphe in sensorimotor processes.

Reward responses

Serotonin is involved in various aspects of reinforcement learning (Ward, Wilkinson et al. 1999; Mobini, Chiang et al. 2000; Cardinal, Winstanley et al. 2004). A large fraction (6 of 13) of putative wide spiking neurons increased their firing rate soon after reward delivery. A subset of neurons also increased firing after reward delivery around the time the water was turned off (Fig. 3-9).

Water valve click response

50% (12 of 24) neurons exhibited a fast response to the click sound of the water valve opening. Latency of response was between 20 and 50 ms with a positive correlation with spike width i.e. wide spiking neurons had latency of 40-50 ms while narrow spiking neurons had response latency of 25 ms (Fig. 3-8). 1 neuron was inhibited by the click.

Tone responsive neurons of similar latency have been observed before in rats as well as cats(Waterhouse, Devilbiss et al. 2004). In our task, the click was immediately followed by the reward delivery. Thus, it is possible that the click was a conditioned reward. Thus, it is difficult to disambiguate if there was a reward component to the click response. In half the behavioral sessions (n= 30 neurons in 13 sessions) the click sound was eliminated and replaced by a pure tone at the time of entry into the goal port. No tone evoked responses were seen in these neurons. The absence of response could be due to differences in stimulus features since click is a broadband stimulus as against a pure tone.

The water valve click can also be considered as a distracting stimulus since the rat does initially during the training startle while drinking. This startle is lost upon training. Serotonin is known to play a role in startle inhibition(Davis, Strachan et al. 1980). Thus the water valve click response may be related to suppressing the startle response to the click. It was observed that 5 of 12 neurons that responded to the click also suppressed firing while in the odor port. These 2 findings are self consistent with role of serotonin in sensorimotor gating since the odor stimulus needs to be attended to, while the valve click needs to be ignored.

Reward timing responses

In all trials, rats had to wait for the water reward after making a response into the correct goal port. This waiting time was either a fixed distribution or drawn from an exponential distribution. Individual rats were well trained with a particular waiting time distribution and hence had a clear temporal expectation of reward. Also, when reward was withheld on a small proportion of randomly interleaved correct responses, there was a negative prediction error (i.e. outcome worse than expected). Thus, by comparing firing rate around time of expected reward delivery we could assess the temporal aspect of the reward signal. By comparing firing rates between rewarded and unrewarded trials, we could assess if the neuron modulates its activity according to the error in prediction. We found that 14 neurons showed modulation around the time of reward. 4 types of responses were seen from time of entry into the goal port to expected time of reward; namely phasic response at the expected time of reward, sustained response, monotonic increase, and decrease of firing rate up to the time of expected reward (Fig. 3-10). No quantitative analysis has been performed to corroborate these observations. Fig 3-10A shows a neuron that increases its firing rate around the time of reward, after which in the unrewarded trials, firing rate remains constant (n=1). Fig. 3-10B shows the opposite trend, where firing decreases up to time of reward (n =3). In Fig 3-10C, firing rate stays constant until just before time of reward, after which in unrewarded trials, firing rate decreases. In Fig 3-10D, there is an exponential distribution of reward delays, with a mean delay of 0.5 sec. In unrewarded trials, there is an abrupt response with a peak of 0.7 sec. Thus, the firing of this neuron correlates with the mean time of expected reward. These examples indicate that raphe neurons may encode reward timing, a signal that is essential in computations of temporal devaluation of rewards.

Differential response to reward omission

In the context of reinforcement learning, serotonin has been proposed to encode aversive or negative reinforcement. In our task, reward was withheld on a small proportion of correct responses thereby leading to a mild disappointment. On these unrewarded trials the rats waited at the goal port until the time of expected reward. This indicates that they had an internal representation of the time of reward delivery.

In a small subset of neurons (n=7), we observed differential firing on rewarded and unrewarded trials immediately after time of reward delivery, independent of the immediate water valve click response. Example rasters and PSTHs are shown in Fig. 3-11. Panels A & B show examples of neurons where firing rate increases immediately after time of expected reward. On the other hand in panel C, the reward delay is exponentially distributed. Thus, although reward is likely at any time point, half the rewards occur within 0.7 sec. Thus, the animal may have a subjective expectation of reward occurrence around this time. In the raster plot in Fig. 3-11 C, trials are grouped into reward omitted trials and those where reward was delayed (> 1.6 sec). These trials show a phasic response around 0.7 sec (also see Fig. 3-10 D) and also another peak around 1.6 sec. This peak is missing in the group of trials where reward occurs early. Thus, we interpret the first response as a reward timing signal and the second as a disappointment signal. While these correlations of firing patterns are interesting, we are aware that there are also other possibilities. For e.g. there may be some correlation of the firing pattern with licking. We have not explicitly tested this possibility.

Task inhibition

4 neurons showed inhibition of firing during all epochs of the task. 3 of the neurons decreased firing upon odor port entry and increased firing upon exit from the water port (Fig. 3-12). 1 neuron showed regular firing during the baseline however, showed marked inhibition when the rat started performing the task. Firing rate increased only when the rat stopped doing the task. This neuron also responded to orienting stimuli outside the task such as suddenly opening the door of the recording chamber. These neurons may be purely encoding the state of the animal. For e.g. they may be inhibited while the animal is engaged in a purposeful behavior. Nevertheless, these responses are intriguing.

Response profile of wide spiking putative serotonin neurons

As discussed in Chapter 2, basic firing properties of wide spiking putative serotonin neurons were heterogeneous. Similarly, there was diversity in responses seen in wide spiking neurons. The most common response was an increase in firing rate after water valve onset. The strongest response was to the click of the water valve with up to 6 fold increase in firing rate. There was one instance of odor selective response and one instance of direction selectivity. During the odor sampling epoch, same number of neurons were inhibited as well as excited. Figure 3-13 summarizes response properties of wide spiking putative serotonin neurons. Four out of 12 wide spiking neurons that fit the criteria for putative serotonin neurons also showed varied response profiles.

A heterogeneous response profile of wide spiking neurons was not expected from the diversity of firing properties of these neurons. There was no response that was preferentially observed in or excluded from wide spiking

neurons. The presence of direction and odor selectivity is surprising since this suggests that serotonin neurons may have very narrow tuning. Six wide spiking neurons responded to reward with a phasic increase in firing rate. This is contrary to expectations from reinforcement learning models of serotonin function(Daw, Kakade et al. 2002) which posit the role of the aversive system or punishment signal to serotonin. However, it should be noted that there is no conclusive evidence that these wide spiking neurons are indeed serotonergic. Three neurons also showed differential firing during unrewarded trials. Of these two neurons decreased their firing rate after omission of reward, while the third increased. The ones that showed suppression also decreased their firing during sleep epochs while the other did not. This supports a view of functional heterogeneity of serotonin neurons that may in some cases correlate with basic firing patterns. On the other hand the 3 burst firing wide spiking neurons had diverse response profiles.

Figure 3-1: odor discrimination task

(A) Behavioral apparatus. Cartoon representation of the behavior box. The box has three recesses called ports, the center odor port and left and right goal ports.

(B) Trial timeline. Events are represented as blips. A trial is initiated by the rat by poking his nose into the odor port. After a random period ranging from 300 – 500 msec, odor is delivered through the odor port. Upon making a decision the rat pulls out of the odor port and makes a movement to one of the goal ports. If the rat makes a correct response, after an anticipation period, the water valve is activated and ~20 μl of water is delivered into the goal port. After a variable time of drinking, the rat moves away from the goal port and the trial is terminated. After a fixed inter-trial-interval, the rat can initiate the next trial.

(C) Behavioral epochs. Cartoon representation of 4 phases of the task. Initiation includes initiation of trial and waiting for odor delivery. Stimulus epoch is the phase in the trial when the rat smells the odor and is inside the odor port. Movement epoch is defined from time of exit from odor port to entry into goal port. Reward epoch includes the anticipation and reward consumption period.

(D) Rats perform the task at a fast speed with stereotyped movements. The two plots are distributions of odor sampling time and movement time for 1 session. Mainen 2003.

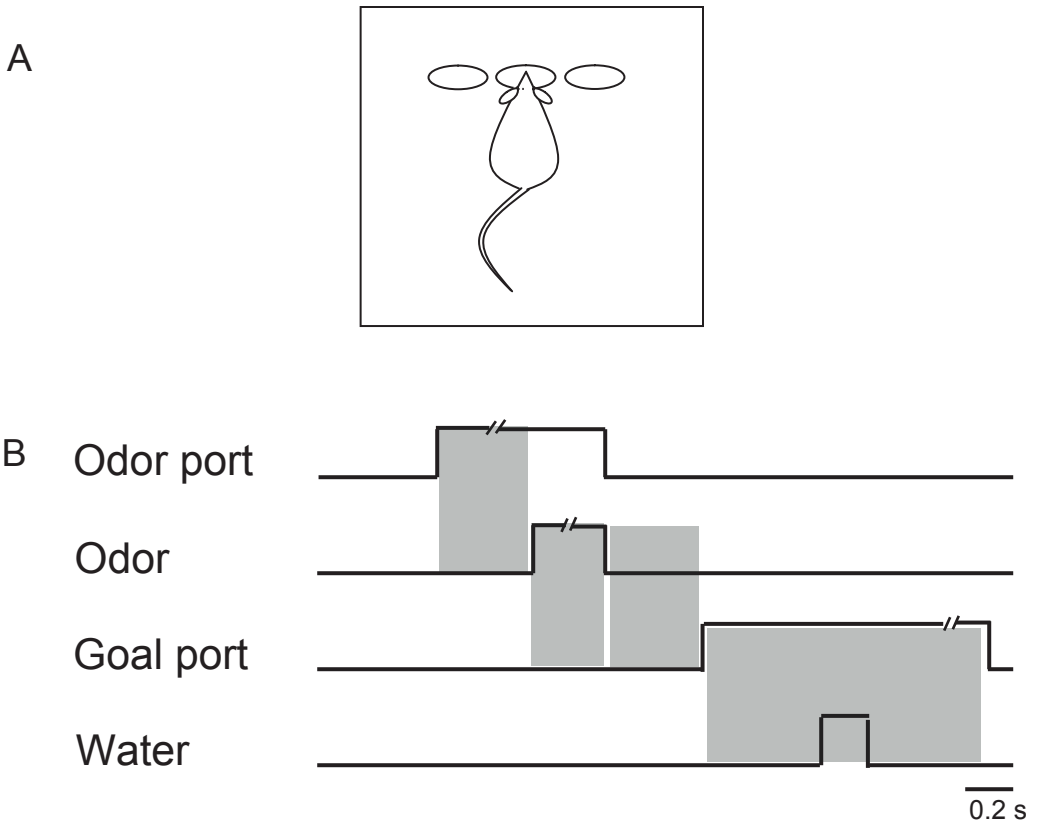
A
B
Odor port
Odor
Goal port
Water
0.2 s
C
L
O
R
Initiation
Stimulus
Movement
Reward
D
mean OSD = 0.39 s
No. of trials
Odor sampling duration (sec)
mean MT = 0.82 s
No. of trials
Movement time (sec)

Figure3-2: Responses during odor sampling

(A) Examples of odor port modulated neuron. Rasters are plotted for 40 representative trials drawn systematically from all valid trials in chronological order. Spikes are aligned to the time of entry into the odor port (Time = 0, yellow line). Blue ticks on rasters indicate onset of odor valve. Dotted green line is the average firing rate of the neuron during the task period.

(left panel) Odor port inhibited neuron. Firing rate of this neuron decreases as the rat enters the odor port, during the delay period and extends into the odor sampling period. Note: firing rate goes to zero upon odor onset.

(Right panel) shows neuron whose firing rate increases upon odor port entry.

(B) Spike width and odor port modulation are not correlated. Scatter plot of spike width vs ROC modulation index (see ROC analysis) for all neurons. Green dots represent cells that are significantly positively modulated ($P<0.05$) during odor port entry (Top Right panel) while red dots represent negatively modulated cells (Top left panel). Arrows indicate the position of cells whose rasters are plotted in the top panels.

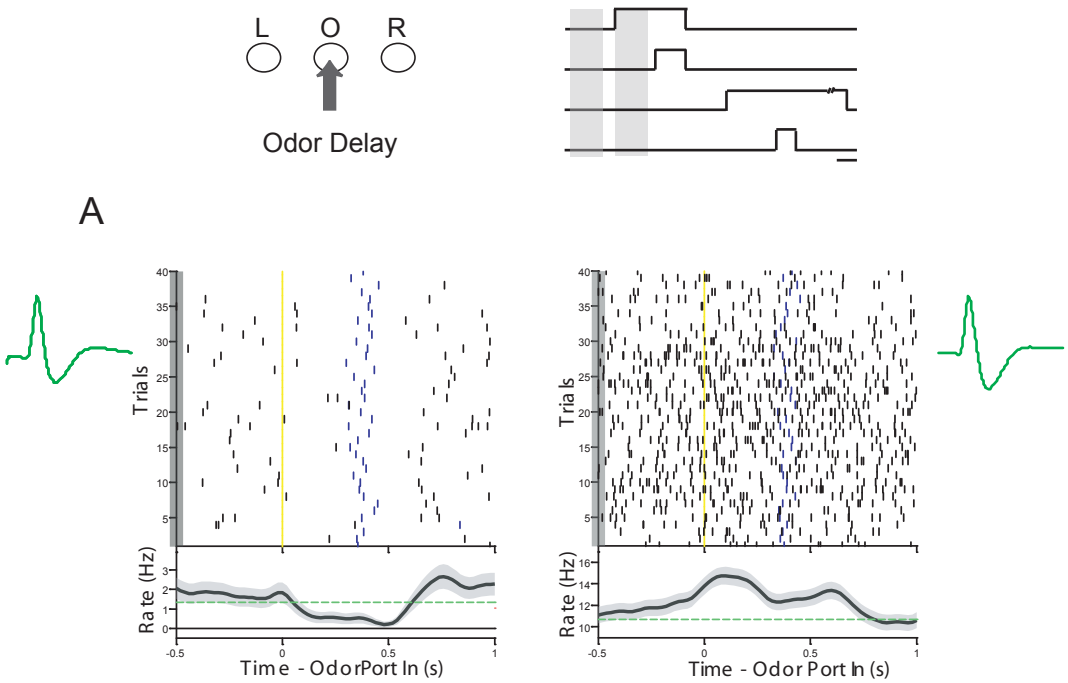
L
O
R
Odor Delay
A
Trials
Rate (Hz)
Time - OdorPort In (s)
Trials
Rate (Hz)
Time - Odor Port In (s)

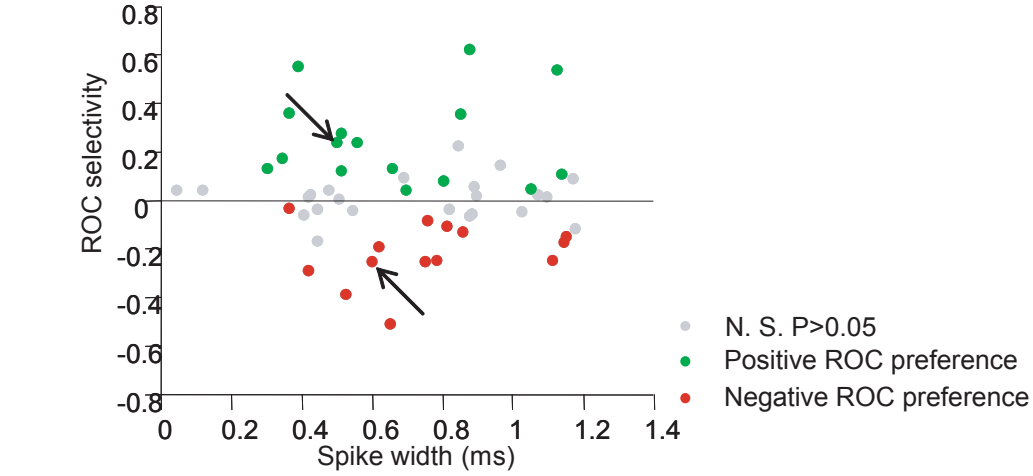
B
ROC selectivity
Spike width (ms)
N. S. P>0.05
Positive ROC preference
Negative ROC preference

Figure 3-3: Odor evoked responses

Example of neuron that modulates its activity upon odor onset. Rasters are plotted for 40 representative trials grouped according to stimulus identity and aligned to onset of the odor valve (Time = 0, yellow line). Within each stimulus trials are sorted by the duration of odor sampling (blue line, Odor port exit time).

(A) Example neuron showing increase in firing rate upon odor presentation. Response latency is ~200 ms.

(B) Neuron with a fast odor onset response. Latency of response is 40 ms. Raster on right is of the same cell at higher time resolution (-0.1 to 0.4 sec) in order to see the latency of the response.

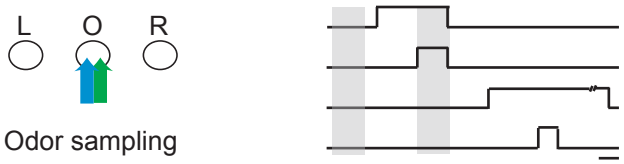
L
O
R
Odor sampling

A

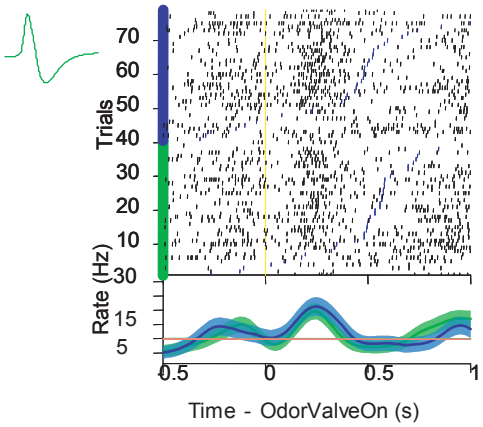
Trials
70
60
50
40
30
20
10
Rate (Hz)
30
15
5
0.5
0
0.5
1
Time - OdorValveOn (s)

B

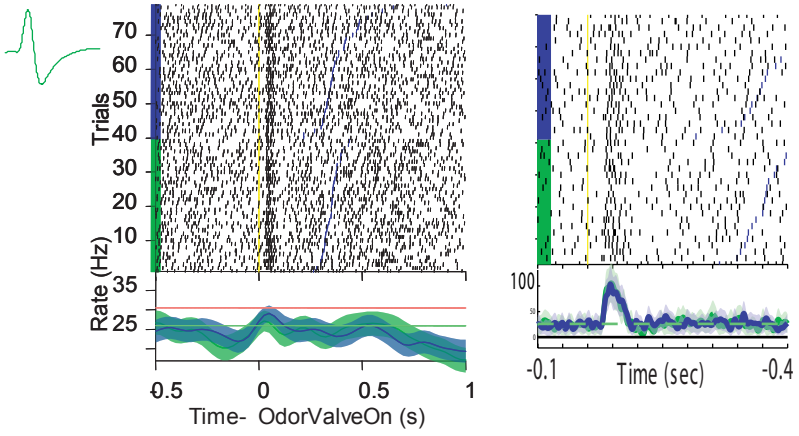
Trials
70
60
50
40
30
20
10
Rate (Hz)
35
25
0.5
0
0.5
1
Time- OdorValveOn (s)
100
-0.1
Time (sec)
-0.4

Figure 3-4: Odor selective response

Examples of neurons showing odor selectivity. Rasters are plotted for 40 representative trials grouped according to stimulus identity and aligned to onset of the odor valve (Time = 0, yellow line). Within each stimulus trials are sorted by the duration of odor sampling (blue line, Odor port exit time).

(A) Example of a neuron showing increase in firing rate upon presentation of 1 odor and inhibition in trials where odor B was presented. Response latency is ~200 ms.

(B) Example of a wide spiking putative serotonin neuron showing odor selective response to odor A and no modulation of firing to odor B. Response latency is ~200ms.

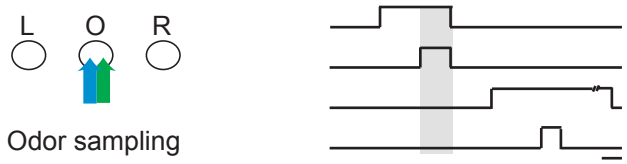
L
O
R
Odor sampling

A

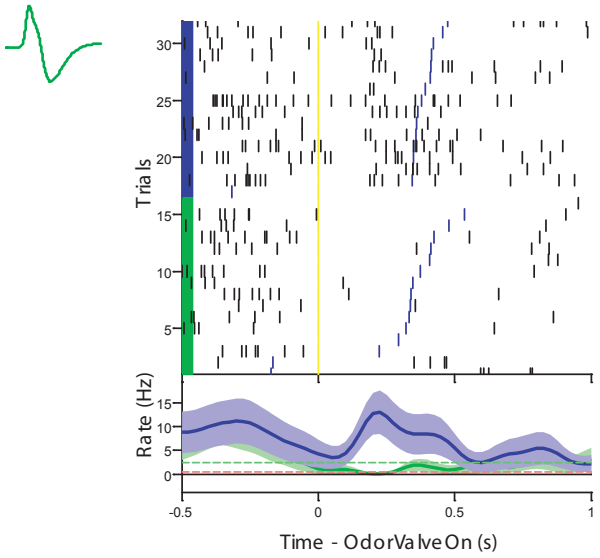
Trials
Rate (Hz)
Time - OdorValveOn (s)

B

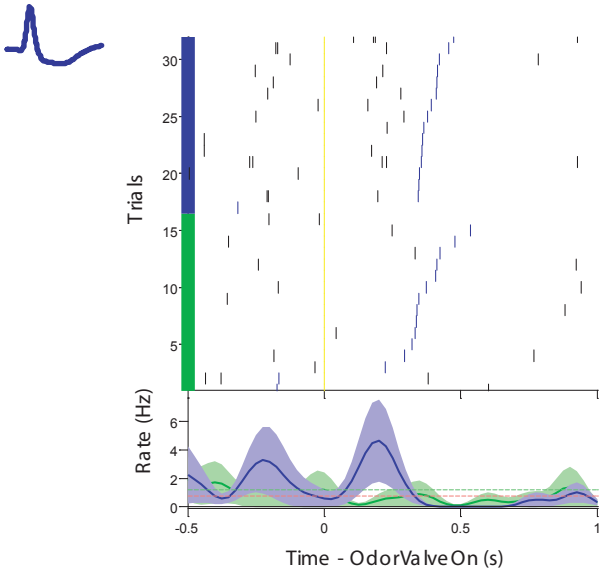
Trials
Rate (Hz)
Time - OdorValveOn (s)

Figure 3-5: Responses during movement out of the odor port

A subset of neurons responded during movement from odor port to the goal port.

(A) Examples of neurons showing a movement response. Rasters plotted with 40 representative trials are aligned to exit from the odor port and sorted by the entry into the goal port. Left panel shows a neuron that increases its firing rate during movement. Right panel shows a neuron that is inhibited during movement.

(B) ROC modulation index plotted as a function of spike width. There was no correlation between spike width and modulation strength. Significant values ($P< 0.05$) are plotted in color. Red points show increase in firing while green points show inhibition during movement.

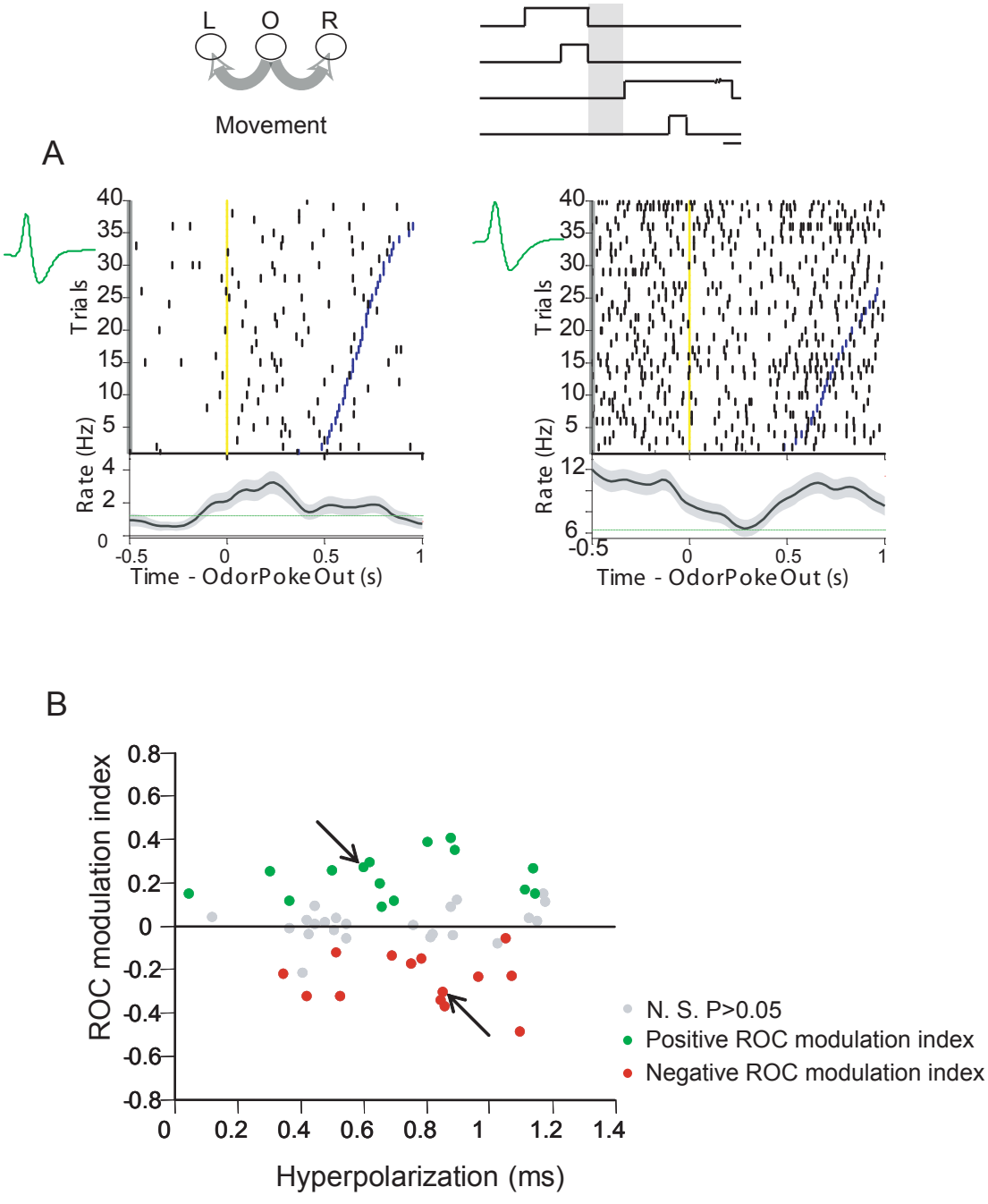
L
O
R
Movement
A
Trials
Rate (Hz)
Time - OdorPokeOut (s)
B
ROC modulation index
Hyperpolarization (ms)
N. S. P>0.05
Positive ROC modulation index
Negative ROC modulation index

Figure 3-6: Direction selective response

A subset of neurons responded selectively to the direction of movement from odor port to the goal port.

(A) Examples of neurons showing a left direction response. Rasters plotted with 40 representative trials are aligned to exit from the odor port and sorted by the entry into the goal port. The neuron increases its firing rate during leftward movement and is inhibited during rightward movement.

(B) Examples of neurons showing a right direction response. The neuron increases its firing rate during rightward movement and is inhibited during leftward movement.

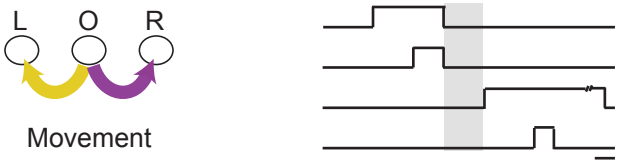
L
O
R
Movement

A

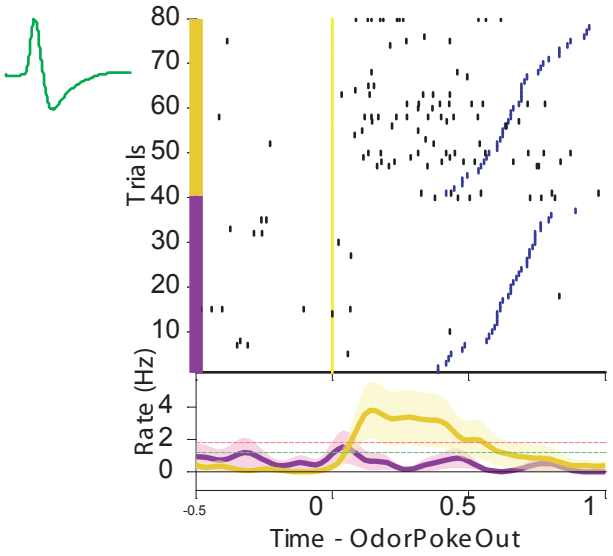
Trials
Rate (Hz)
Time - OdorPokeOut

B

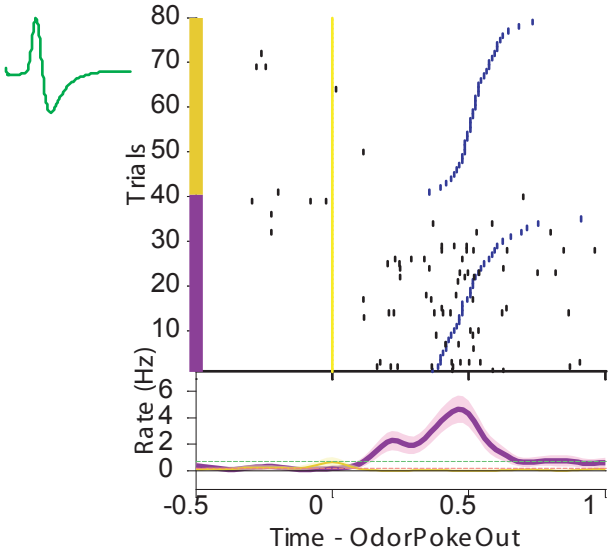
Trials
Rate (Hz)
Time - OdorPokeOut

Figure 3-7: Odor sampling response and movement response are anti-correlated

A large fraction (n = 30) were significantly anti-correlated during odor sampling and movement.

(A) Examples of neurons showing opposite tuning during odor sampling and movement. Rasters are plotted for each neuron aligned (time = 0, yellow line) to the time of odor port entry and to the time of the odor port exit. Trials are placed in order of occurrence from bottom to top and sorted by movement time in the 2 rasters respectively. Left panel shows example of a neuron that was inhibited during odor sampling but showed an increase in firing rate to movement. Right panel shows an example of a neuron with the opposite tuning. Green dotted lines on the PSTHs are mean firing rates during the task.

(B) Comparison of ROC modulation index at odor port entry and odor port exit.

ROC values were calculated by comparing firing rates during epochs of length 300ms before and after odor port entry and exit. Arrows indicate ROC values of neurons plotted in the rasters in (A).

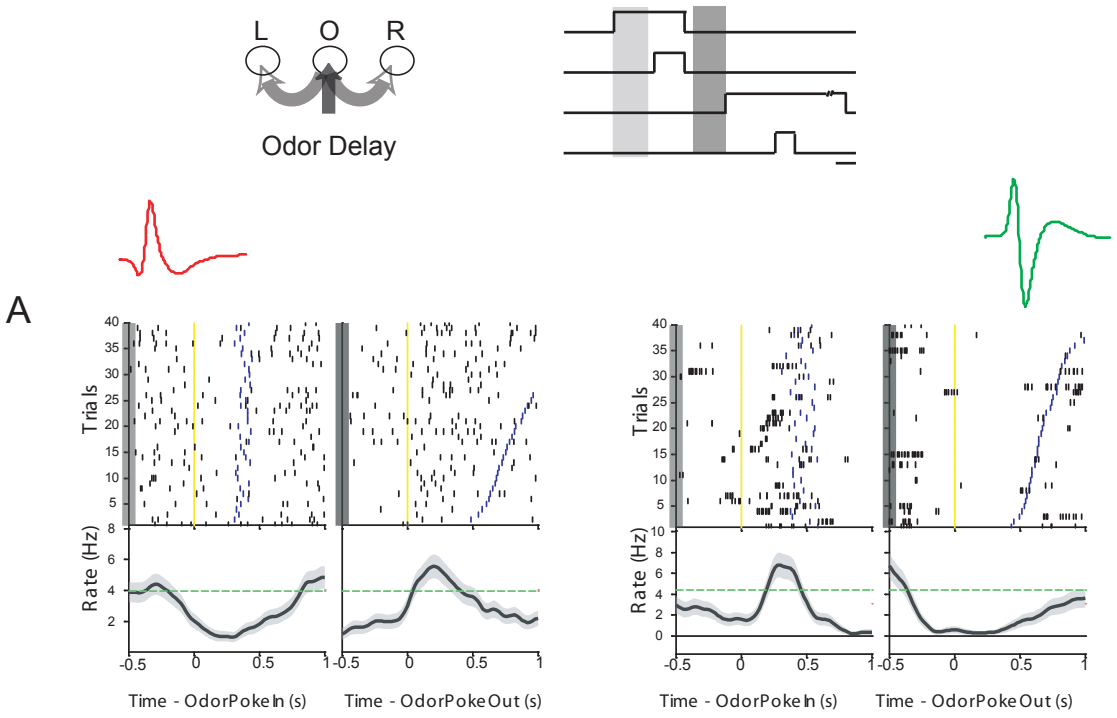
L
O
R
Odor Delay
A
Trials
Rate (Hz)
Time - OdorPokeIn (s)
Time - OdorPokeOut (s)
Time - OdorPokeIn (s)
Time - OdorPokeOut (s)

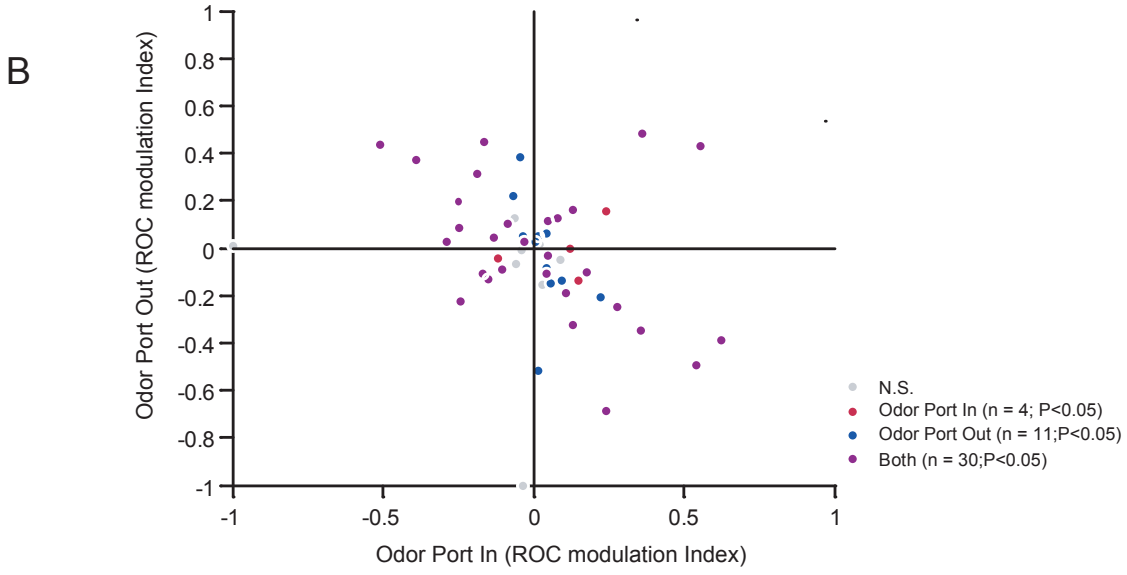
B
Odor Port Out (ROC modulation Index)
Odor Port In (ROC modulation Index)
N.S.
Odor Port In (n = 4; P<0.05)
Odor Port Out (n = 11;P<0.05)
Both (n = 30;P<0.05)

Figure 3-8: Response to the click of the water valve

12 of 24 neurons responded to the sound of the water valve click. A,B, and C show rasters plotted with 40 representative trials, aligned to the onset of the water valve (time = 0, yellow line). Trials are sorted by the water valve open time. Dark blue ticks denote time of turning off the water valve.

(A) Response of a wide spiking neuron to the water valve click. Response latency is around 50 ms.

(B) Response of a narrow spiking neuron to the water valve click. Response latency is around 20 ms.

(C) Only one neuron showed a specific inhibition in response to the water valve click. Latency of inhibition is ~20 ms.

(D) Linear correlation between response latency and spike width (hyperpolarization). Median latencies for wide spiking neurons were 50 ms while for symmetric neurons it was 25ms.

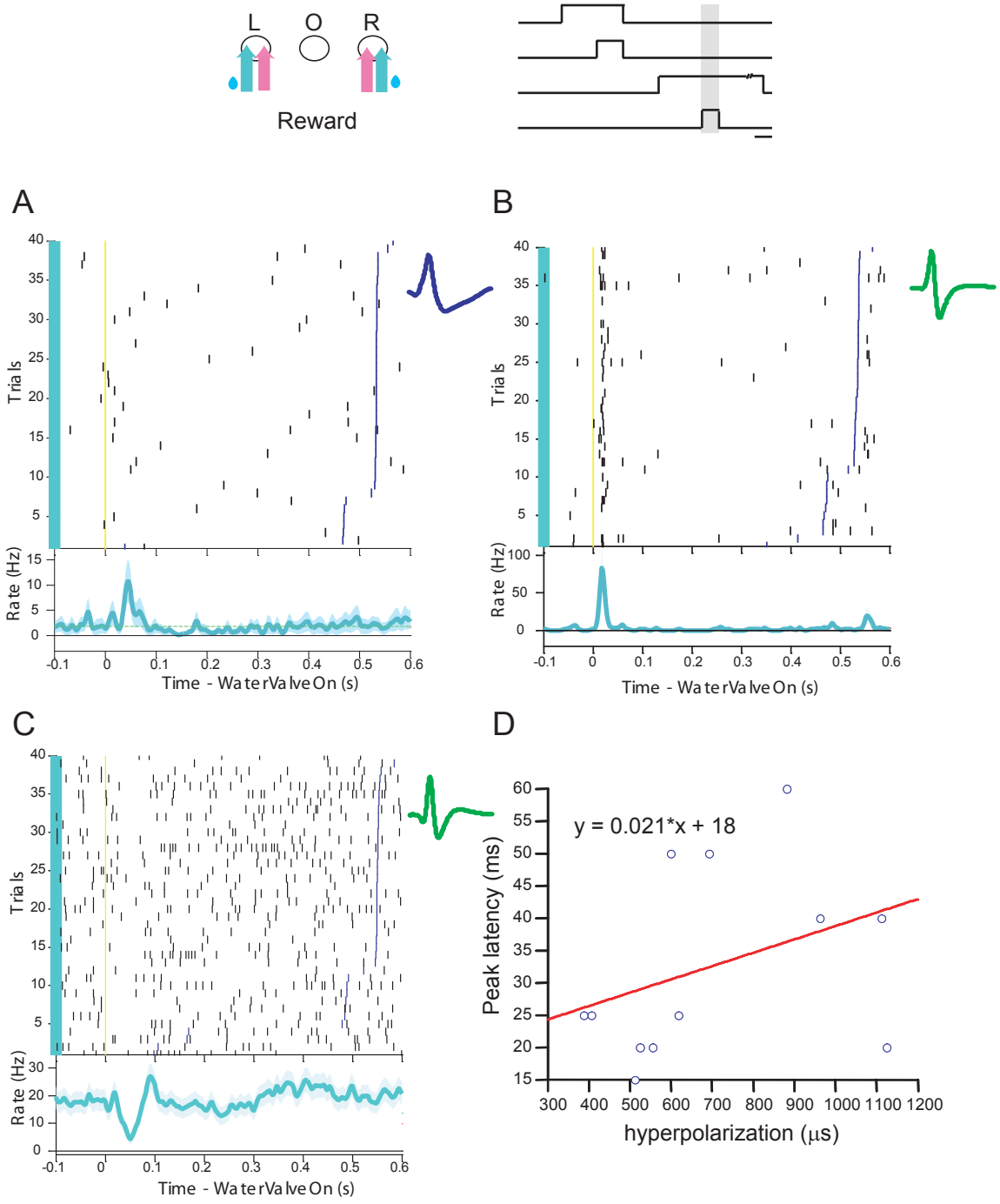
L
O
R
Reward
A
B
C
D
Trials
Rate (Hz)
Time - WaterValveOn (s)
Peak latency (ms)
hyperpolarization (μs)
y = 0.021*x + 18

Figure 3-9: Response during drinking

Neurons responded during drinking with either an increase or a decrease in firing. Predominant response was an inhibition during drinking. Examples of neurons with a drinking response are shown. Rasters are plotted with 40 representative trials aligned to water valve onset (yellow line; time = 0) and sorted by valve open time. Dark blue ticks correspond to closing of the water valve.

(A) shows a neuron that increases its firing rate while drinking while (B) shows a neuron that decreases firing during drinking.

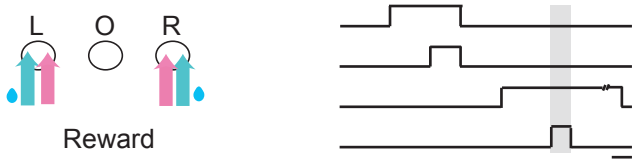
L
O
R
Reward

A

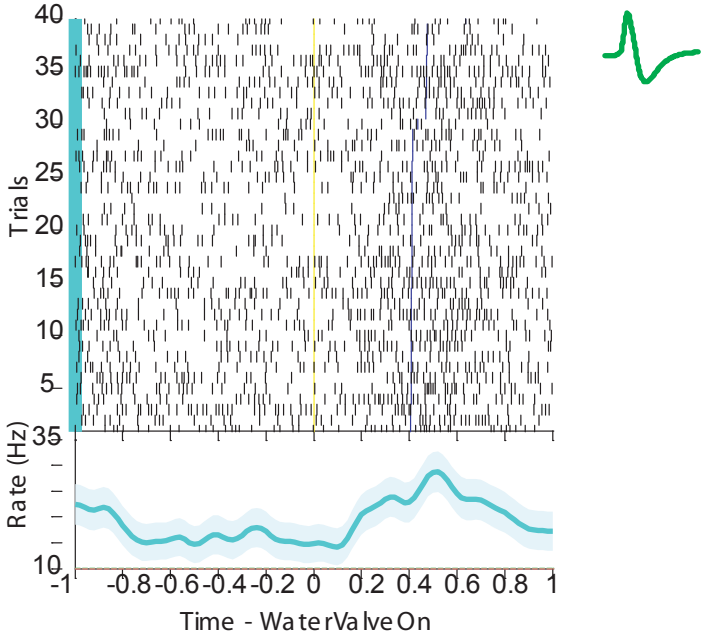
Trials
Rate (Hz)
Time - WaterValveOn

B

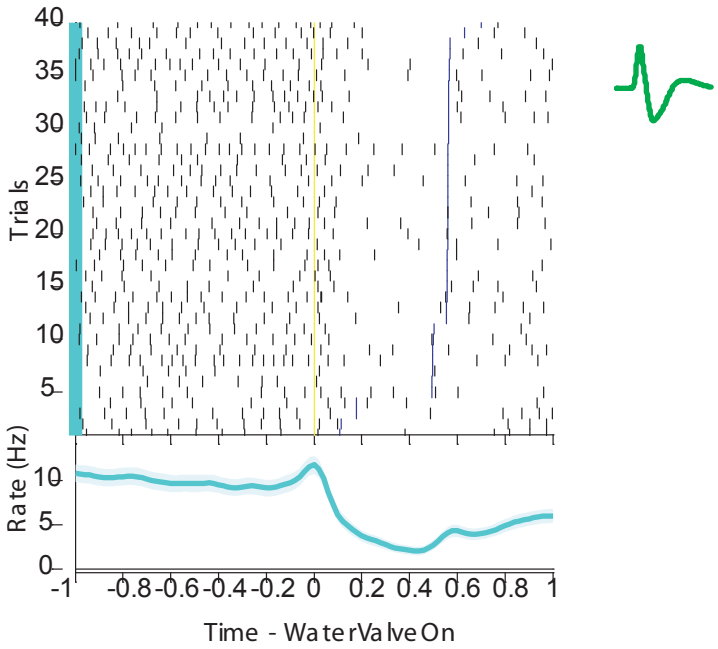
Trials
Rate (Hz)
Time - WaterValveOn

Figure 3-10: Responses to timing of reward

A small subset of neurons responded to the timing of reward delivery. Rasters are plotted for 40 representative trials, aligned to entry into the water port. Cyan sidebar indicates rewarded trials and pink indicates unrewarded correct trials. All trials are sorted by the timing of exit from the water port. Water drop in the PSTH denotes time of expected reward.

(A) Increase in firing rate at time of reward delivery. This neuron increases its firing rate around time of expected reward. Note: red ticks in raster of unrewarded trials are the water port exit time.

(B) Firing rate of neuron decreases monotonically until time of reward. In rewarded trials there is an offset response while in unrewarded trials inhibition continues until goal port exit.

(C) Decrease in firing rate at time of reward delivery. Firing rate of neuron is sustained throughout the delay and decreases abruptly around time of reward. In rewarded trials it increases after reward while in unrewarded trials it decreases further.

(D) Reward delays for this neuron were exponentially distributed with a median of 0.70 s. Plotted are only correct rewarded trials with delays more than 1.5 sec. and unrewarded trials. Water drop indicates median delay to reward. An abrupt phasic response is seen in both rewarded and unrewarded trials.

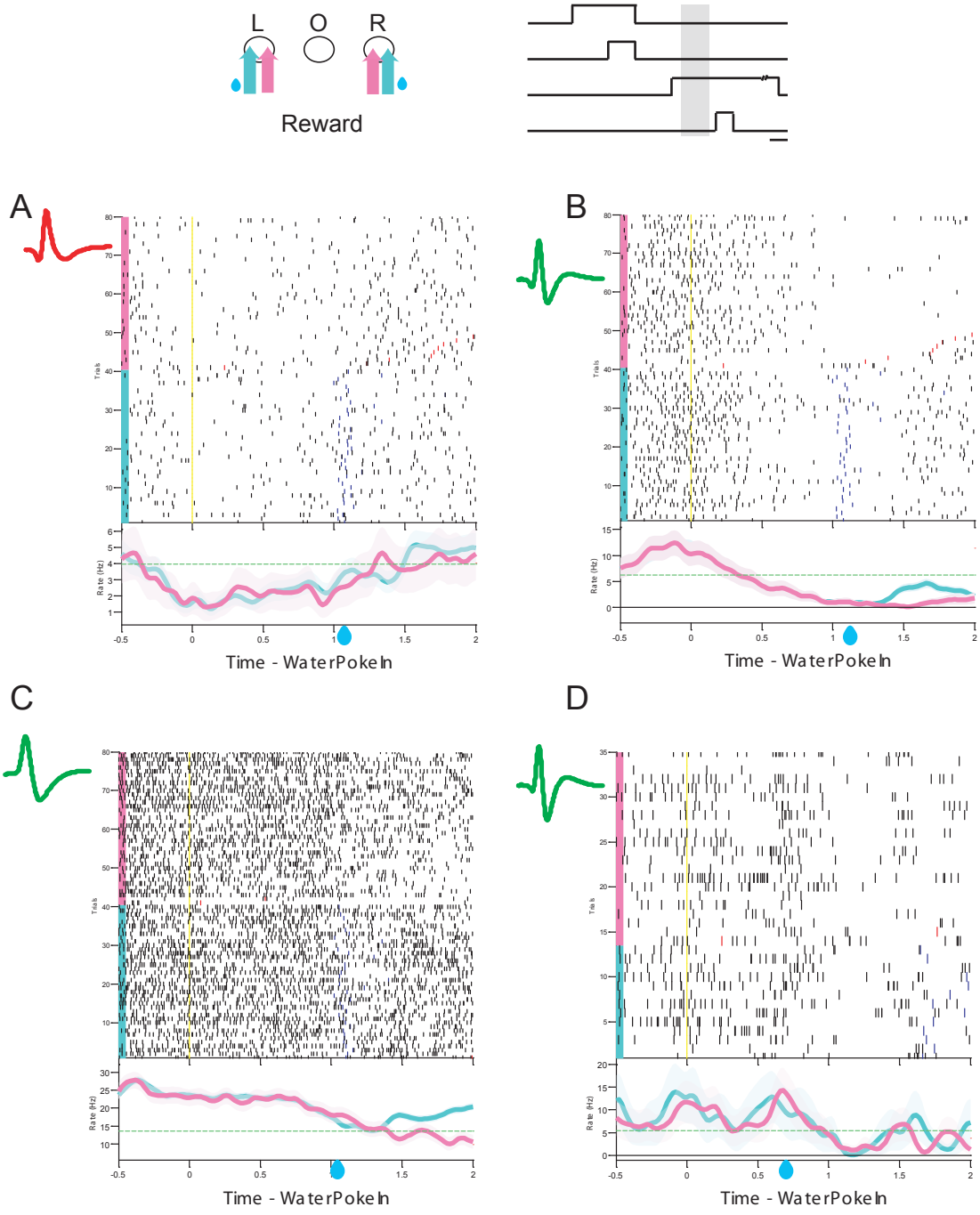
L
O
R
Reward
A
B
C
D
Trials
Rate (Hz)
Time - WaterPokeIn

Figure 3-11: Differential response to reward omission

A small subset of neurons responded to the omission of expected reward. Rasters are plotted for 40 representative trials, aligned to entry into the water port. Cyan sidebar indicates rewarded trials and pink indicates unrewarded correct trials. All trials are sorted by the timing of exit from the water port. Water drop in the PSTH denotes time of expected reward.

(A) & (B) show neurons whose firing rate increases after reward omission. Note that A is a wide spiking neuron.

(C) shows a wide spiking neuron whose firing rate decreases after reward omission.

(D) shows a neuron similar to one shown in Fig. 3-10D. It fires at the median time of expected reward and also just before the maximum reward delay (indicated by water drop).

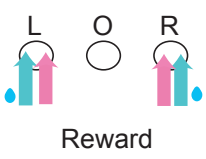
L
O
R
Reward

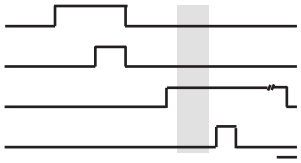

A

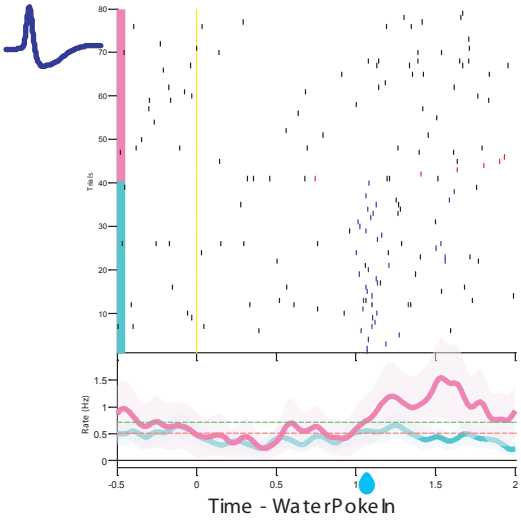
Trials
Rate (Hz)
Time - WaterPokeIn

B

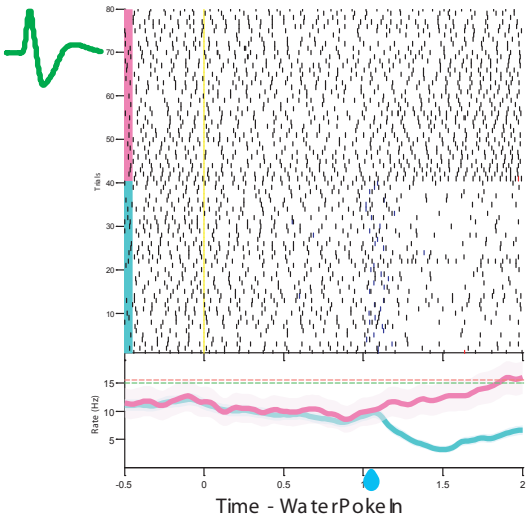
Trials
Rate (Hz)
Time - WaterPokeIn

C

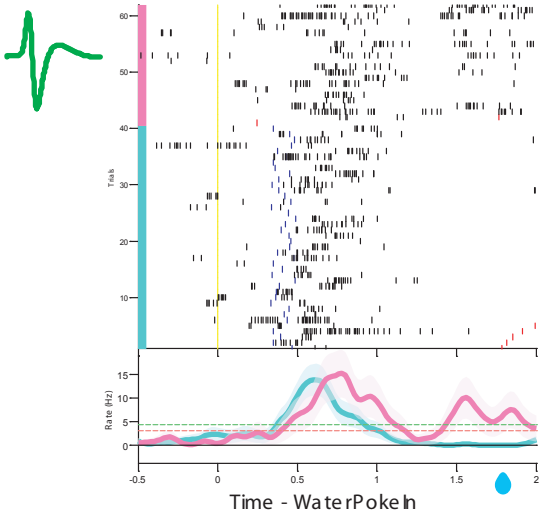
Trials
Rate (Hz)
Time - WaterPokeIn

D

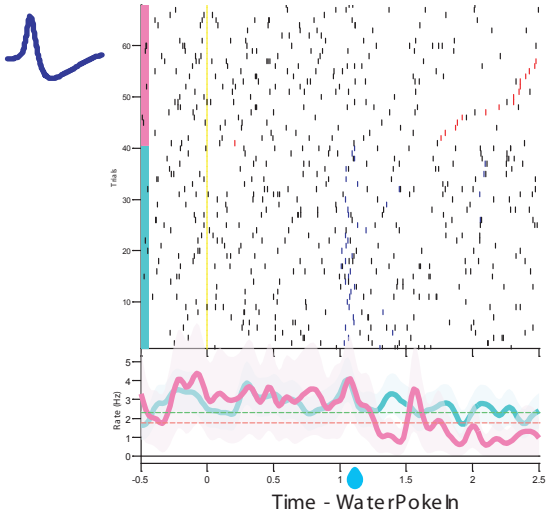
Trials
Rate (Hz)
Time - WaterPokeIn

Figure 3-12: Inhibition of neurons during the task

A small subset of neurons showed inhibition while performing the task. Rasters are plotted for 40 representative trials, aligned on the left to odor port entry and on the right to exit from the water port. The blue ticks are time of odor valve onset.

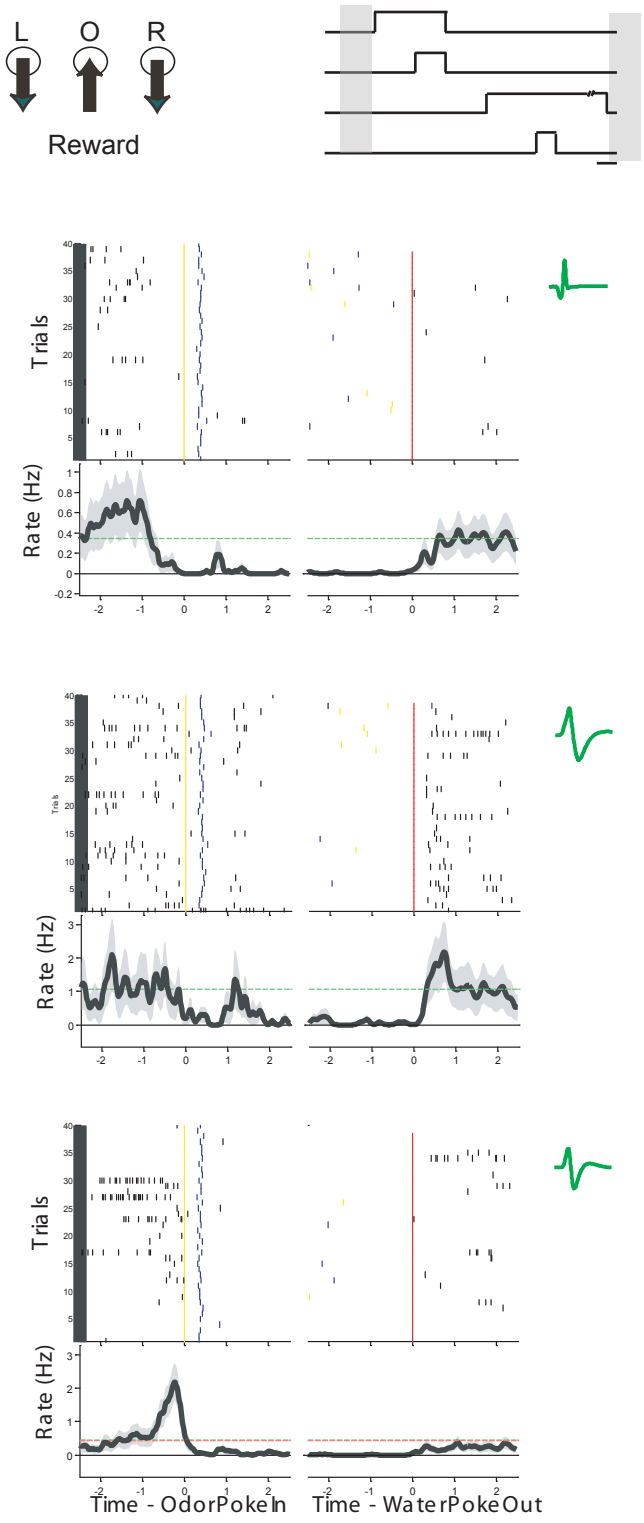
L
O
R
Reward
Trials
Rate (Hz)
Trials
Rate (Hz)
Trials
Rate (Hz)
Time - OdorPokeIn
Time - WaterPokeOut

Figure 3-13: Response summary of wide spiking neurons

Wide spiking putative serotonin neurons responded to a variety of behavioral events. Each column represents a behavioral epoch. + indicates up modulation while – indicates down modulation of firing rates. * indicates odor and direction selective response.

No.	Odor Poke	Odor sampling	Movement	Water valve click	Reward consumption	Reward expectation
1	-	-	+*			+
2					+	
3					+	
4	+			+		
5		-	+		+	
6	+		-			
7	+	-			+	+
8		+*			+	
9	-	-	+	+		
10	+	+	-	+	+	+
11	-		+		+	
12	-	+	+			
13	-		+*			

Conclusions / Perspectives

Summary of main findings

We recorded activity of neurons in the dorsal raphe nucleus (DRN) of rats while they were engaged in a 2-odor discrimination task. We found much diversity in the firing properties of neurons in the DRN with respect to spike waveform shapes, firing rates and regularity of firing and levels or nature of sleep wake modulation. Similarly, while performing the task, raphe neurons responded to all events during the task from odor anticipation, odor sampling, movement and reward anticipation and reward consumption. Response profiles did not segregate with any other firing characteristics e.g. spike width. In fact, cases of identical response profiles were noted for neurons with very different spike waveforms. Responses of wide spiking putative serotonin neurons were also sharply locked to behavioral events. This suggests to us that raphe neurons encode short timescale behavioral events. The most common and robust response was an inhibition of firing during the odor sampling period. These responses provide support to the sensorimotor hypothesis of serotonin function; i.e. raphe is inhibited while attending to a behaviorally relevant sensory stimulus. Similarly, a large proportion of raphe neurons showed a sharp phasic response to the sound of the water valve click. We argue that this response is in relation to the suppression of acoustic startle. Raphe neurons exhibited very narrow response specificity, e.g. odor selective tuning, directional tuning. Raphe neurons also showed responses during reward consumption. A subset of responses was correlated with reward expectation in time as well as differential responses to omission of reward.

Phasic changes in raphe neuron firing, a phasic serotonin signal?

Neuromodulatory systems are believed to have spatially distributed, temporally extended effects on target structures(Doya 2002). Indeed, most studies on serotonin have focused on effects of serotonin on long timescales. Recordings of raphe neuronal firing patterns have also detailed only tonic changes in firing rate while mentioning phasic (short time scale) changes as anecdotes(Fornal, Metzler et al. 1996). Therefore, our finding of abrupt changes in firing rates precisely time locked to behavioral events over the order of milliseconds is significant since it argues for a possible action of serotonin at behavioral time scales.

Response heterogeneity: diverse physiology, diverse function

One of the most striking aspects of the serotonergic raphe system is its high degree of convergence of inputs and widespread divergence of projections to diverse areas in the brain. This suggests that the raphe system is uniquely placed to be influenced by and in turn affect neuronal activity of diverse brain areas. Indeed, serotonin is known to affect a wide range of behaviors and physiological processes. However, recordings from raphe neurons have until date, presented a very different picture. The only responses seen in serotonin neurons in the awake animal are to movement and sleep states(Fornal, Metzler et al. 1996; Waterhouse, Devilbiss et al. 2004). Contrary to these studies we find a tremendous degree of heterogeneity of responses to sensory, movement as well as reward related aspects. The discrepancy arises due to differences in approach. While earlier studies have recorded neuronal activity in the freely behaving animal, in our task rats are engaged in a temporally well controlled behavioral task. Thus, we have better information on the behavior of the rat, both

qualitatively and temporally. Our task is well suited to test responses of neurons in sensory, decision, and reward processes. In addition, we have not applied any pre-selection criteria for neuronal properties, hence we can study the entire, heterogeneous population of raphe neurons. Most importantly, we chose to study the responses of neurons at shorter timescale phasic modulation of firing rates as opposed to long timescale tonic modulation.

More information on recorded neurons

In order to study the raphe nucleus with all its complexity, it is important to obtain as much information as can be obtained from the neurons that are recorded. Information on their neurochemistry, anatomical localization and projections will help to construct specific, testable theories of serotonin function. Therefore, recording approaches need to be complemented with stimulation based or molecular genetic based approach to gain extra bits of information on recorded neurons.

Raphe system may specifically modulate functional circuits

Recent anatomical evidence suggests that there is a level of organization to the inputs and output projections of the raphe nucleus(Abrams, Johnson et al. 2004). An encephalotopic map in the raphe and innervation by single raphe neurons of multiple areas subserving a functional circuit suggest that serotonin release can be under exquisite spatial and temporal control. While we did not see any strong evidence for correlation of response profiles by location in the raphe, our dataset is not suited for such analysis due to relatively low number of neurons as well as lack of fine spatial information on recording sites. Further studies will be required to directly address this issue.

Use of novel behavioral paradigms that address specific function

In order to better understand the function of serotonin, it is imperative to record from raphe neurons in the context of tasks that are known to have deficits due to serotonin dysfunction. This needs to also be combined with manipulations to projection areas that are also involved in the task. Such concerted approach will give more specific information on serotonin function.

Use of mouse as a model organism

In order to fully utilize the potential of molecular genetic tools and knockout technologies mouse is an ideal model system. Recent advances in genetically encoded neuronal activators and inhibitors such as channelrhodopsin and halorhodopsin give us a fine spatiotemporal control on the activity of specific subpopulations of neurons in the raphe. Using these tools we can now investigate the effects of serotonin at short timescales. (Zhang, Aravanis et al. 2007). In order to effectively test specific theories of serotonin function, behavioral paradigms need to be standardized for mice. During my graduate work, I have been able to successfully train mice on a 2-odor discrimination task. Similar results have recently been published by other groups(Rinberg, Koulakov et al. 2006).

Is there a central theory of serotonin function?

Serotonin is a diffuse, highly divergent neuronal projection system. It is indeed tantalizing to think that it computes a single parameter and broadcasts it to the entire brain. On the other hand, it may be that the raphe is indeed modular with small subsets of neurons modulating an entire functional circuit(Lowry 2002). These modules can interact with each other through local interactions and feedback from inputs so as to coordinate their output. In order to get to the

question of a fundamental role of serotonin in the brain, we will have to begin by trying to understand these modules.

Materials and methods

Animal subjects

Male Long Evans rats weighing 250-350 g were used for all experiments. Rats were placed on a 12-hour reversed light cycle to enable experiments during their active phase. Free food was available but water access was restricted to behavior and ½ hour of free access at some other time during the day. Weights were maintained within 85% of free feeding weight. Free food and water was available during the weekend. All procedures involving animals were carried out in accordance with National Institutes of Health standards as approved by the Cold Spring Harbor Laboratory Institutional Animal Care and Use Committee.

Behavioral procedures

All behavioral procedures were conducted as described in Uchida and Mainen 2003. The behavior box, which was built in house, was kept inside a recording chamber. Behavior box had 3 ports; i.e. recesses in the wall, equipped with an infrared photodiode and phototransistor. Interruption of the bean signaled time of entry of rat into the particular port. Analog signals from all ports were recorded simultaneously with digital timestamps. Odors used were (+) and (-) enantiomers of 2-octanol. These were mixed 10 fold in mineral oil and further diluted in air with a custom built olfactometer (Uchida and Mainen 2003). A reward of 20 ◎l was delivered through solenoid valves for correct responses. To minimize the valve click sound of the water delivery system, the valves were kept outside the chamber encased in noise reducing foam for part of the

experiments. Delivery of odors and water reinforcement was actuated by data acquisition hardware (National Instruments) while control software was written in MATLAB.

Tetrode microdrive design

When I joined the lab, tetrode microdrives were built by hand from basic materials like stainless steel tubes and dental acrylic as the molding material. This process was laborious and liable to mistakes. In order to achieve high throughput, I decided to design a microdrive that could be machined. With the help of Rob Eiffert, the machinist at CSHL, we made a drive design suitable for stereolithography or '3-D printing'. This allowed identical drives to be built with minimum manual labor (apart from the electrode loading process). This microdrive was rather inexpensive ($ 150-200) and was hence called the 'budget drive'. Engineering associate Matt Recchia helped in redesigning the drive and outsourcing the 3-D printing. An engineering drawing of the microdrive design is shown in Fig. 2-1. I also designed a smaller, compact drive that would be able to drive a single bundle of tetrodes. The drive was made from 3 very simple machined delrin parts and could be built within 2 hours. A 3-D model of this drive is shown.

Guide cannula implantation

The DRN is located at following coordinates with respect to bregma -0.76 AP, 0.0 Lateral, and 5.0mm DV according to Paxinos and Watson, 5th Edition. This location is exactly at the confluence of the sagittal and transverse sinuses. Therefore, due to the bleeding, it is not possible to target the tetrodes directly to the DRN vertically from the top. We employed an approach used by other groups (Guzman-Marin, Alam et al. 2000; Waterhouse, Devilbiss et al. 2004) to

record from DRN, which involves implanting a guide cannula into the brain and lowering the microdrive through it. A cartoon of the guide cannula implantation is shown in Fig 2-1. The guide cannula used was made out of a 18.5 Ga thin walled stainless steel tubing encased in a delrin housing.

Surgical implantation of tetrode drive assembly

Rats were anesthetized with a solution of ketamine and medetomidine. The head was shaved and positioned in the stereotax using atraumatic ear bars. The skin above the skull was retracted and the skull surface cleaned. A hole was drilled in the skull above the raphe at -7.8 posterior to bregma and the thinned skull was gently removed. The underlying sinus was punctured using a fine gauge needle and guide cannula with the dummy cannula inside it was pierced through the sinus. The guide cannula was fixed to the skull with dental acrylic and the dummy cannula was removed. If there was blood in the guide cannula, it was removed with a wick. The tetrode drive was then lowered through the guide cannula to a depth of 3mm below the surface. The drive was fixed to the skull, ground, EEG and hippocampal EEG electrodes were placed and the skin was sutured or retracted back. The animal was give Ketofen as a analgesic and left to recover. Temperature was kept constant during surgery using a heat blanket. Al wounds were irrigated with lidocaine. Animal was allowed to recover for a week before starting water deprivation.

Tetrode recordings

Extracellular recordings were carried out using a 4-6 tetrode microdrive described earlier. Tetrodes were made be twisting and fusing together 4, 12 μm polyimide coated nichrome wires. DiI, a fluorescent marker was coated onto the outside of the tetrode to facilitate viewing the tracks. Typical impedance of

tetrodes was brought to 250-500 KΩ by gold plating. Electrical signals were amplified on a unity gain op- amp preamplifier connected to the microdrive on the rat and transferred to programmable amplifiers (Cheetah acquisition system, Neuralynx, Tucson, AZ) via flexible, shielded cables. Sampling rate was set at 32 KHz, band-pass filtered from 0.3-6KHz. Thresholds were set on individual channels so that anytime the voltage crossed threshold on 1 of the channels, an event was defined. The waveform of this event was captured in 32 sample points around it, amplified 5000-80000 times and stored to disk using the Cheetah software acquisition system. Timestamps of all events were also stored. Recordings were obtained for a total of 2-3 weeks as electrodes were lowered everyday to sample new populations of neurons. While lowering the electrodes, distance traversed was noted from the number of turns (1 turn = 320 micron) of the screw.

Histology

At the end of the experiment, rats were deeply anesthetized until all reflexes were completely lost. Electrical lesions were made at the end of each tetrode by applying a 30 μA DC current for 5-10 sec with the ground connected to the animal. The rat was perfused transcardiacally, initially with ~ 100 ml of chilled 0.9 % saline, followed by ~ 300ml of chilled 4% paraformaldehyde (PFA) solution in PBS. After perfusion, fixed brains were carefully extracted from the skull and preserved in 4% PFA. Thin, 50 μm sections were cut on a vibratome and mounted on slides or kept in wells filled with saline. Sections containing the tracks were photographed along with micrometer scale and recording location were backtracked from the site of the lesion (Fig 2-1).

Spike sorting

Spike sorting was done offline using MCLUST software (A.D. Redish). Manual clustering was based on spike features measured from the spike waveform. The concept behind spike sorting is similar to triangulation, where spike features from 4 channels of the tetrode are slightly different and therefore separate into distinct clusters of points when plotted against one another. Initially principal features such as peak, valley and energy were used to roughly separate spike sources. The clusters were further refined using derived quantities such as the first principal component of the waveform, FFT. Only cells with very few refractory period violations were accepted (Fig 2-2).

Calculation of ROC modulation index

Modulation is operationally defined as a significant change in firing rate compared to baseline. A unit/cell/neuron was considered to modulate its activity during a given epoch if the firing rate distribution during the epoch was distinguishable from the baseline firing rate distribution using ROC analysis. The ROC ('receiver operator characteristic') analysis (Green and Swets, 1966) originated in signal detection theory and has been widely used as a metric to define neuronal responses ((Britten, Shadlen et al. 1992). The area under the ROC curve (AUC) is a direct measure of the discriminability of the two signals, and is related to the overlap of the two underlying distributions. AUC ranges from 0 to 1, where 1 and 0 are situations where the two distributions are perfectly discriminable with opposite signs, while 0.5 is a situation where the two distributions perfectly overlap. Thus, in the case of modulation strength with respect to two behavioral epochs, 1 represents scenario where firing rate in the test epoch is always higher than the firing rate in the reference (baseline) epoch. 0

is the opposite where the firing rate is always lower than the reference. We derived a more intuitive measure from the AUC measure, and named it the ROC modulation index (Feierstein, Quirk et al. 2006).

$$\text{ROC modulation index} = 2.(\text{ROCarea} - 0.5)$$

This yields a measure that ranges from -1 to 1, where 1 means firing rate is always higher than reference epoch, while -1 means inhibition of firing and 0 means no change.

Bootstrap significance estimate

Significance of ROC modulation index was estimated using bootstrapping. 200 bootstraps were typically performed to estimate significance of $P<0.05$.

References

Abrams, J. K., P. L. Johnson, et al. (2004). "Anatomic and functional topography of the dorsal raphe nucleus." Ann N Y Acad Sci **1018**: 46-57.

Adell, A., P. Celada, et al. (2002). "Origin and functional role of the extracellular serotonin in the midbrain raphe nuclei." Brain Res Brain Res Rev **39**(2-3): 154-80.

Aghajanian, G. K. and C. P. Vandermaelen (1982). "Intracellular identification of central noradrenergic and serotonergic neurons by a new double labeling procedure." J Neurosci **2**(12): 1786-92.

Aghajanian, G. K. and R. Y. Wang (1977). "Habenular and other midbrain raphe afferents demonstrated by a modified retrograde tracing technique." Brain Res **122**(2): 229-42.

Allers, K. A. and T. Sharp (2003). "Neurochemical and anatomical identification of fast- and slow-firing neurones in the rat dorsal raphe nucleus using juxtacellular labelling methods in vivo." Neuroscience **122**(1): 193-204.

Araneda, S., K. Gysling, et al. (1999). "Raphe serotonergic neurons projecting to the olfactory bulb contain galanin or somatostatin but not neurotensin." Brain Res Bull **49**(3): 209-14.

Britten, K. H., M. N. Shadlen, et al. (1992). "The analysis of visual motion: a comparison of neuronal and psychophysical performance." J Neurosci **12**(12): 4745-65.

Cardinal, R. N., C. A. Winstanley, et al. (2004). "Limbic corticostriatal systems and delayed reinforcement." Ann N Y Acad Sci **1021**: 33-50.

Dahlstrom, A. and K. Fuxe (1964). "Localization of monoamines in the lower brain stem." Experientia **20**(7): 398-9.

Davis, M., D. I. Strachan, et al. (1980). "Excitatory and inhibitory effects of serotonin on sensorimotor reactivity measured with acoustic startle." Science **209**(4455): 521-3.

Daw, N. D., S. Kakade, et al. (2002). "Opponent interactions between serotonin and dopamine." Neural Netw **15**(4-6): 603-16.

Doya, K. (2002). "Metalearning and neuromodulation." Neural Netw **15**(4-6): 495-506.

Feierstein, C. E., M. C. Quirk, et al. (2006). "Representation of spatial goals in rat orbitofrontal cortex." Neuron **51**(4): 495-507.

Fornal, C. A., C. W. Metzler, et al. (1996). "A subgroup of dorsal raphe serotonergic neurons in the cat is strongly activated during oral-buccal movements." Brain Res **716**(1-2): 123-33.

Guzman-Marin, R., M. N. Alam, et al. (2000). "Discharge modulation of rat dorsal raphe neurons during sleep and waking: effects of preoptic/basal forebrain warming." Brain Res **875**(1-2): 23-34.

Hajos, M., K. A. Allers, et al. (2007). "Neurochemical identification of stereotypic burst-firing neurons in the rat dorsal raphe nucleus using juxtacellular labelling methods." Eur J Neurosci **25**(1): 119-26.

Hajos, M., S. E. Gartside, et al. (1995). "Evidence for a repetitive (burst) firing pattern in a sub-population of 5-hydroxytryptamine neurons in the dorsal and median raphe nuclei of the rat." Neuroscience **69**(1): 189-97.
Hajos, M., C. D. Richards, et al. (1998). "An electrophysiological and neuroanatomical study of the medial prefrontal cortical projection to the midbrain raphe nuclei in the rat." Neuroscience **87**(1): 95-108.
Harrison, A. A., B. J. Everitt, et al. (1999). "Central serotonin depletion impairs both the acquisition and performance of a symmetrically reinforced go/no-go conditional visual discrimination." Behav Brain Res **100**(1-2): 99-112.
Ho, M. Y., D. N. Velazquez-Martinez, et al. (2002). "5-Hydroxytryptamine and interval timing behaviour." Pharmacol Biochem Behav **71**(4): 773-85.
Hollerman, J. R. and W. Schultz (1998). "Dopamine neurons report an error in the temporal prediction of reward during learning." Nat Neurosci **1**(4): 304-9.
Imai, H., D. A. Steindler, et al. (1986). "The organization of divergent axonal projections from the midbrain raphe nuclei in the rat." J Comp Neurol **243**(3): 363-80.
Jacobs, B. L. and E. C. Azmitia (1992). "Structure and function of the brain serotonin system." Physiol Rev **72**(1): 165-229.
Jacobs, B. L., S. L. Foote, et al. (1978). "Differential projections of neurons within the dorsal raphe nucleus of the rat: a horseradish peroxidase (HRP) study." Brain Res **147**(1): 149-53.
Jacobs, B. L. and C. A. Fornal (1991). "Activity of brain serotonergic neurons in the behaving animal." Pharmacol Rev **43**(4): 563-78.
Jacobs, B. L. and C. A. Fornal (1997). "Serotonin and motor activity." Curr Opin Neurobiol **7**(6): 820-5.
Jacobs, B. L. and C. A. Fornal (1999). "Activity of serotonergic neurons in behaving animals." Neuropsychopharmacology **21**(2 Suppl): 9S-15S.
Kalen, P., M. Karlson, et al. (1985). "Possible excitatory amino acid afferents to nucleus raphe dorsalis of the rat investigated with retrograde wheat germ agglutinin and D-[3H]aspartate tracing." Brain Res **360**(1-2): 285-97.
Kalen, P., G. Skagerberg, et al. (1988). "Projections from the ventral tegmental area and mesencephalic raphe to the dorsal raphe nucleus in the rat. Evidence for a minor dopaminergic component." Exp Brain Res **73**(1): 69-77.
Kirouac, G. J., S. Li, et al. (2004). "GABAergic projection from the ventral tegmental area and substantia nigra to the periaqueductal gray region and the dorsal raphe nucleus." J Comp Neurol **469**(2): 170-84.
Kocsis, B., V. Varga, et al. (2006). "Serotonergic neuron diversity: identification of raphe neurons with discharges time-locked to the hippocampal theta rhythm." Proc Natl Acad Sci U S A **103**(4): 1059-64.
Kocsis, B. and R. P. Vertes (1992). "Dorsal raphe neurons: synchronous discharge with the theta rhythm of the hippocampus in the freely behaving rat." J Neurophysiol **68**(4): 1463-7.
Kosofsky, B. E. and M. E. Molliver (1987). "The serotoninergic innervation of cerebral cortex: different classes of axon terminals arise from dorsal and median raphe nuclei." Synapse **1**(2): 153-68.

Levine, E. S. and B. L. Jacobs (1992). "Neurochemical afferents controlling the activity of serotonergic neurons in the dorsal raphe nucleus: microiontophoretic studies in the awake cat." J Neurosci **12**(10): 4037-44.

Lowry, C. A. (2002). "Functional subsets of serotonergic neurones: implications for control of the hypothalamic-pituitary-adrenal axis." J Neuroendocrinol **14**(11): 911-23.

Mamounas, L. A. and M. E. Molliver (1988). "Evidence for dual serotonergic projections to neocortex: axons from the dorsal and median raphe nuclei are differentially vulnerable to the neurotoxin p-chloroamphetamine (PCA)." Exp Neurol **102**(1): 23-36.

Mamounas, L. A., C. A. Mullen, et al. (1991). "Dual serotoninergic projections to forebrain in the rat: morphologically distinct 5-HT axon terminals exhibit differential vulnerability to neurotoxic amphetamine derivatives." J Comp Neurol **314**(3): 558-86.

McGinty, D. J. and R. M. Harper (1976). "Dorsal raphe neurons: depression of firing during sleep in cats." Brain Res **101**(3): 569-75.

Mirenowicz, J. and W. Schultz (1994). "Importance of unpredictability for reward responses in primate dopamine neurons." J Neurophysiol **72**(2): 1024-7.

Mobini, S., T. J. Chiang, et al. (2000). "Effects of central 5-hydroxytryptamine depletion on sensitivity to delayed and probabilistic reinforcement." Psychopharmacology (Berl) **152**(4): 390-7.

Molliver, M. E. (1987). "Serotonergic neuronal systems: what their anatomic organization tells us about function." J Clin Psychopharmacol **7**(6 Suppl): 3S-23S.

Monckton, J. E. and D. A. McCormick (2002). "Neuromodulatory role of serotonin in the ferret thalamus." J Neurophysiol **87**(4): 2124-36.

Mosko, S. S., D. Haubrich, et al. (1977). "Serotonergic afferents to the dorsal raphe nucleus: evdience from HRP and synaptosomal uptake studies." Brain Res **119**(2): 269-90.

Peyron, C., J. M. Petit, et al. (1998). "Forebrain afferents to the rat dorsal raphe nucleus demonstrated by retrograde and anterograde tracing methods." Neuroscience **82**(2): 443-68.

Rinberg, D., A. Koulakov, et al. (2006). "Speed-accuracy tradeoff in olfaction." Neuron **51**(3): 351-8.

Sakai, K. and S. Crochet (2001). "Differentiation of presumed serotonergic dorsal raphe neurons in relation to behavior and wake-sleep states." Neuroscience **104**(4): 1141-55.

Schultz, W. and R. Romo (1990). "Dopamine neurons of the monkey midbrain: contingencies of responses to stimuli eliciting immediate behavioral reactions." J Neurophysiol **63**(3): 607-24.

Sprouse, J. S. and G. K. Aghajanian (1987). "Electrophysiological responses of serotoninergic dorsal raphe neurons to 5-HT1A and 5-HT1B agonists." Synapse **1**(1): 3-9.

Tork, I. (1990). "Anatomy of the serotonergic system." Ann N Y Acad Sci **600**: 9-34; discussion 34-5.

Trulson, M. E. and T. Crisp (1986). "Do serotonin-containing dorsal raphe neurons possess autoreceptors?" Exp Brain Res **62**(3): 579-86.

Trulson, M. E. and B. L. Jacobs (1979). "Raphe unit activity in freely moving cats: correlation with level of behavioral arousal." Brain Res **163**(1): 135-50.
Ungerstedt, U. (1971). "Stereotaxic mapping of the monoamine pathways in the rat brain." Acta Physiol Scand Suppl **367**: 1-48.
Urbain, N., K. Creamer, et al. (2006). "Electrophysiological diversity of the dorsal raphe cells across the sleep-wake cycle of the rat." J Physiol **573**(Pt 3): 679-95.
Veasey, S. C., C. A. Fornal, et al. (1995). "Response of serotonergic caudal raphe neurons in relation to specific motor activities in freely moving cats." J Neurosci **15**(7 Pt 2): 5346-59.
Veasey, S. C., C. A. Fornal, et al. (1997). "Single-unit responses of serotonergic dorsal raphe neurons to specific motor challenges in freely moving cats." Neuroscience **79**(1): 161-9.
Vertes, R. P. (1991). "A PHA-L analysis of ascending projections of the dorsal raphe nucleus in the rat." J Comp Neurol **313**(4): 643-68.
Ward, B. O., L. S. Wilkinson, et al. (1999). "Forebrain serotonin depletion facilitates the acquisition and performance of a conditional visual discrimination task in rats." Behav Brain Res **100**(1-2): 51-65.
Waterhouse, B. D., D. Devilbiss, et al. (2004). "Sensorimotor-related discharge of simultaneously recorded, single neurons in the dorsal raphe nucleus of the awake, unrestrained rat." Brain Res **1000**(1-2): 183-91.
Zhang, F., A. M. Aravanis, et al. (2007). "Circuit-breakers: optical technologies for probing neural signals and systems." Nat Rev Neurosci **8**(8): 577-81.